

Performance Prediction for Large-Scale Nuclear Waste Repositories: Final Report

*W. E. Glassley, J. J. Nitao, C. W. Grant, T. N. Boulos, M.
O. Gokoffski, J. W. Johnson, J. R. Kercher, J. A. Levatin,
and C. I. Steefel*

February 1, 2001

U.S. Department of Energy

Lawrence
Livermore
National
Laboratory

DISCLAIMER

This document was prepared as an account of work sponsored by an agency of the United States Government. Neither the United States Government nor the University of California nor any of their employees, makes any warranty, express or implied, or assumes any legal liability or responsibility for the accuracy, completeness, or usefulness of any information, apparatus, product, or process disclosed, or represents that its use would not infringe privately owned rights. Reference herein to any specific commercial product, process, or service by trade name, trademark, manufacturer, or otherwise, does not necessarily constitute or imply its endorsement, recommendation, or favoring by the United States Government or the University of California. The views and opinions of authors expressed herein do not necessarily state or reflect those of the United States Government or the University of California, and shall not be used for advertising or product endorsement purposes.

This work was performed under the auspices of the U. S. Department of Energy by the University of California, Lawrence Livermore National Laboratory under Contract No. W-7405-Eng-48.

This report has been reproduced directly from the best available copy.

Available electronically at <http://www.doc.gov/bridge>

Available for a processing fee to U.S. Department of Energy
And its contractors in paper from
U.S. Department of Energy
Office of Scientific and Technical Information
P.O. Box 62
Oak Ridge, TN 37831-0062
Telephone: (865) 576-8401
Facsimile: (865) 576-5728
E-mail: reports@adonis.osti.gov

Available for the sale to the public from
U.S. Department of Commerce
National Technical Information Service
5285 Port Royal Road
Springfield, VA 22161
Telephone: (800) 553-6847
Facsimile: (703) 605-6900
E-mail: orders@ntis.fedworld.gov
Online ordering: <http://www.ntis.gov/ordering.htm>

OR

Lawrence Livermore National Laboratory
Technical Information Department's Digital Library
<http://www.llnl.gov/tid/Library.html>

Performance Prediction For Large-Scale Nuclear Waste Repositories: Final Report

William. E. Glassley, Principal Investigator

John J. Nitao, Technical Lead

Participants: Charles W. Grant, Thomas N. Boulos, Mary O.
Gokoffski, James W. Johnson, James R. Kercher, Jo Anne Levatin,
and Carl I. Steefel,

Tracking Code: 98-SI-004

February, 2001

TABLE OF CONTENTS

I.	SYNOPSIS	1
II.	INTRODUCTION AND PROJECT PURPOSE	2
III.	ACTIVITIES ACCOMPLISHED	4
	Description of NUFT-C capabilities	5
	Performance on the ASCI Blue Pacific IBM SP-2	7
IV.	VALIDATION	8
	Plug Flow Reactor Experiments	8
	Drift-Scale Test	10
	Yucca Mountain Pore Waters	14
V.	TECHNICAL OUTCOME	20
	Application to a Potential High Level Nuclear Waste Repository	20
	Chemical and physical processes important for long term performance	22
	Chemical and physical processes important for post-closure monitoring	26
	Other Applications	32
VI.	SUMMARY	39
VII.	ACKNOWLEDGEMENTS	40
VIII.	REFERENCES	41
IX.	PUBLICATIONS	42

I. SYNOPSIS

The goal of this project was development of a software package capable of utilizing tera-scale computational platforms for solving subsurface flow and transport problems important for disposal of high level nuclear waste materials, as well as for DOE-complex clean-up and stewardship efforts. We sought to develop a tool that would diminish reliance on abstracted models, and realistically represent the coupling between subsurface fluid flow, thermal effects and chemical reactions that both modify the physical framework of the rock materials and which change the rock mineralogy and chemistry of the migrating fluid. Providing such a capability would enhance realism in models and increase confidence in long-term predictions of performance. Achieving this goal also allows more cost-effective design and execution of monitoring programs needed to evaluate model results.

This goal was successfully accomplished through the development of a new simulation tool (NUFT-C). This capability allows high resolution modeling of complex coupled thermal-hydrological-geochemical processes in the saturated and unsaturated zones of the Earth's crust. The code allows consideration of virtually an unlimited number of chemical species and minerals in a multi-phase, non-isothermal environment. Because the code is constructed to utilize the computational power of the tera-scale IBM ASCI computers, simulations that encompass large rock volumes and complex chemical systems can now be done without sacrificing spatial or temporal resolution. The code is capable of doing one-, two-, and three-dimensional simulations, allowing unprecedented evaluation of the evolution of rock properties and mineralogical and chemical change as a function of time.

The code has been validated by comparing results of simulations to laboratory-scale experiments, other benchmark codes, field scale experiments, and observations in natural systems. The results of these exercises demonstrate that the physics and chemistry embodied in the code accurately represents the state-of-the-art in modeling these processes, and that the conceptualization of the models used in the simulations honors the primary processes that are controlling these systems.

Application of the code to a wide range of important and strategic problems has been undertaken. Particularly significant are results obtained concerning the evolution of a potential high level nuclear waste repository at Yucca Mountain, Nevada. In these simulations, the results suggest that fluid movement and chemical changes will be such as to encourage solute transport around the sides of the waste emplacement tunnels, thus minimizing the potential for seepage of water and dissolved salts into the tunnels. The results also indicate that the short term response of the geological system to waste emplacement will be complex and rapid, and will be most readily detected below waste emplacement tunnels. A successful monitoring program of repository performance during the early stages of the operational period would thus benefit by coordinating design and execution of sampling strategies with a simulation tool such as NUFT-C. Such an approach would allow efficient and cost-effective sampling strategies, and would facilitate interpretation of what will surely be complex and massive data sets.

II. INTRODUCTION AND PROJECT PURPOSE

One of the major challenges faced by the Department of Energy in its efforts to accomplish site clean-up and long term disposal of high level nuclear waste, is to acquire the ability to realistically model and predict movement of fluids in the subsurface. Such a capability is necessary in order to achieve confidence that the performance of sites will satisfy regulatory requirements, and to assure that adequate stewardship of sites, through long-term monitoring and performance confirmation activities, can be achieved.

This is a challenging problem because the ability to conduct realistic simulations of subsurface flow and transport has historically been limited by the intense computational demand such simulations place on computer systems. Such simulations commonly require that fluid movement, chemical reactions under non-isothermal conditions, and evolving properties of the physical framework through which flow occurs, be addressed simultaneously (Figure 1). Historically, realistic solutions to such problems was hampered because simulations required tera-byte computational resources, when only giga-byte resources were available. The strategy that was then followed was to address each part of the problem separately (e.g., conduct separate simulations of thermal-hydrological processes in a static physical framework, and chemical processes in a fully saturated condition in a static flow field), and develop abstraction tools to combine the results.

The recent development of the ASCI massively parallel computational platforms with tera-byte computational power has dramatically changed the simulation landscape, now making it possible to conduct the large scale simulations needed to address these problems.

The goal of the project described in this document was to develop software capable of utilizing the tera-scale machines for simulations of subsurface flow and transport problems. We sought to develop a tool that would diminish reliance on abstracted models, and realistically represent the coupling between subsurface fluid flow, thermal effects and chemical reactions that both modify the physical framework of the rock materials and which change the rock mineralogy and chemistry of the migrating fluid. This tool would include the ability to consider an unlimited number of chemical species in solution and mineral species composing the rock, and a large number of different types of rock materials. It would also be capable of doing two-dimensional and three-dimensional simulations, encompassing large areas and volumes of rock (cubic kilometers), while maintaining representation of the relevant processes at high resolution. These goals were successfully accomplished.

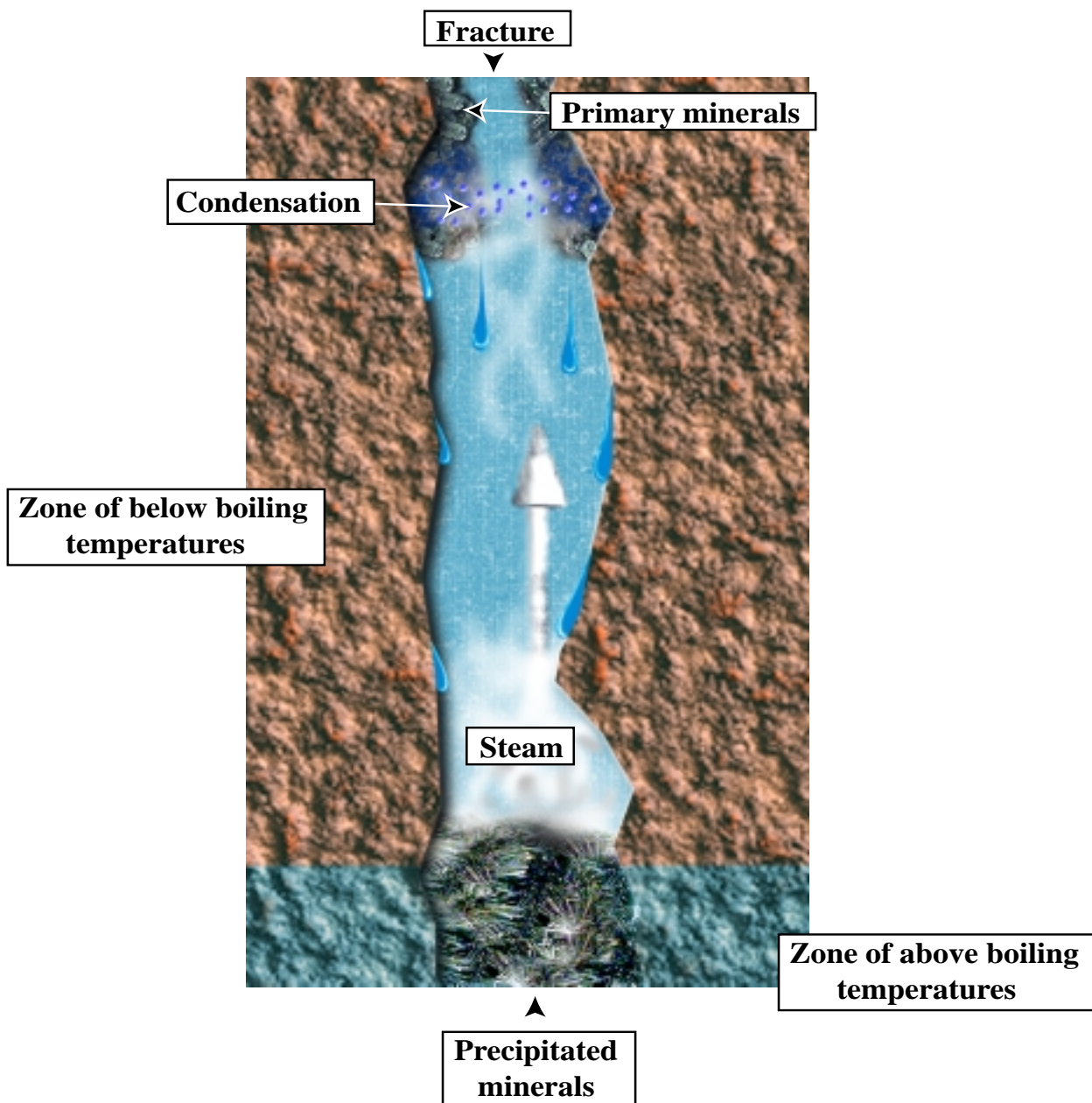


Figure 1: Schematic representation of coupled thermal-hydrological-geochemical interactions represented in NUFT-C. In this schematic, a fracture cuts through porous rock that exists within the unsaturated zone at some unspecified depth where the local boiling temperature is exceeded in rock in the lower portion of the diagram. At the boiling front, steam forms and migrates to lower pressure and lower temperature conditions, where it condenses and flows back toward the boiling front under the influence of gravity. In the region where condensation occurs, primary minerals present on the fracture surface are partially dissolved, as are minerals in the porous rock along the flow path of the migrating water. The resulting dissolved load is carried in the condensed water back to the boiling front where the dissolved load is precipitated as a new suite of secondary minerals, thus modifying the size and shape of the fracture opening. Not shown are similar processes that are simultaneously occurring within the matrix of the porous rock. NUFT-C rigorously represents the chemistry and physics necessary to model this system.

III. ACTIVITIES ACCOMPLISHED

The activities completed under this Strategic Initiative resulted in development and application of the world's most powerful tool for simulating coupled thermal-hydrological-geochemical processes within saturated and unsaturated media. Using the high performance IBM ASCI Blue Pacific massively parallel computer, this code was applied to a wide range of problems, including the only 3-dimensional, high resolution simulations ever done of 10's to 100 waste packages in a potential high level nuclear waste repository in unsaturated rocks. Applications in the areas of carbon sequestration, geothermal systems and nuclear waste repositories in saturated environments were also completed.

The new reactive transport code, NUFT-C, was built upon the thermal-hydrological computational capabilities of the code NUFT (Nitao, 1998). NUFT (Nonisothermal Unsaturated-Saturated Flow and Transport model) is a suite of multi-phase, multicomponent models for numerical solution of non-isothermal flow and transport in porous media with application to subsurface contaminant-transport problems. Modules in the code allow simulations of unconfined and confined saturated flow, single-phase unsaturated flow (Richard's equation), single-component contaminant transport, and multi-phase, multi-component flow and transport with non-isothermal conditions. These distinct models are imbedded in a single code to utilize a common set of utility routines and input file format.

An integrated, finite-difference, spatial discretization is used to solve the relevant balance equations for heat and mass transfer. The resulting nonlinear equation is solved at each time step by the Newton-Raphson method.

To accomplish the goal of developing a reactive transport simulator, the capabilities described below were added to NUFT to allow kinetically controlled dissolution and precipitation reactions with feedback to the thermal-hydrological system. Account is taken of how the structure of the rock changes in response to the dissolution and precipitation reactions, and how this impacts the permeability field.

The code allows representation of any number of geological rock units. These units are represented as distinct hydrological and mineralogical entities with discrete properties (see Figure 1 for a schematic representation of this conceptualization). Simulations can be done in either an equivalent continuum mode, or a dual porosity/dual permeability mode. For homogeneous media, a single continuum approach is used, while a fracture continuum and a matrix continuum can be defined for fractured rock units. In the dual continuum approach, interaction between the two continua is determined by user-specified parameters that include such things as the abundance of fractures and the exposed surface area of the fractures per unit cell area or unit volume.

A built-in mesh generator provides the code with the capability to construct a computational mesh based on user defined domain ranges. The domains can consist of individual rock units or collections of units that share similar properties. Distribution of data for each domain among the processors is accomplished by decomposing the computational domain into logically rectangular collections of cells, with cell dimensions being user defined.

Chemical properties of the system are determined by the rock and fracture mineralogies (mineral volume fractions) and pore gas and water compositions. The number of minerals and aqueous species that can be used in any given simulation is only limited by machine capacity.

Currently, the code runs on the Unix and DOS operating systems. Versions have been successfully compiled and tested for IBM-PC compatibles, Cray Unicos, and Sun, Hewlett-Packard, IBM Risc/6000, Silicon Graphics, and DEC Alpha workstations.

Provided immediately below is a more detailed description of the capabilities of NUFT-C.

Description of NUFT-C capabilities

Aqueous speciation reactions. Reactions are computed on the basis of thermodynamic data supplied by the user. Activity coefficients for the aqueous species are computed using the extended Debye-Huckel method. It is assumed that reactions maintain thermodynamic equilibrium. Dissolved gas species are also included, accounting for equilibrium thermodynamic exchange between liquid and coexisting gases. An unlimited number of aqueous species can be considered. The thermodynamic database used for computing mass action relationships can be from any source. The databases we have employed are those currently supported within the GEMBOCHS package (Johnson and Lundeen, 1994 a,b, 1995)

Mineral dissolution and precipitation reactions. Dissolution of existing minerals, or precipitation of saturated and supersaturated mineral species are represented by kinetic equations of the form used in transition state theory. Thermodynamic data needed for these calculations is derived from similar sources as those described above for the aqueous species. Descriptions of mineral abundance, and the effective reactive surface areas of each mineral phase in each rock unit can be used to represent mineral evolution. The volume of each mineral phase dissolved or precipitated at each time step, and its consequence for the porosity of the rock at each cell of the computational mesh is computed. This change in porosity is the basis for establishing the time varying permeability evolution of the rock units. Mineral precipitation can be treated as a kinetic process equivalent to the negative rate of the respective mineral phase dissolution, or as a power function of that rate, thus allowing account to be taken of the experimentally observed differences in mineral dissolution and precipitation kinetics. Changes in mineral abundance can be made dependent on solution properties, consistent with transition state theory, allowing a predetermined degree of supersaturation to be achieved if so desired.

Explicit representation of fracture and matrix mineralogy. Use of a dual continuum model allows the mineralogies and pore water and gas chemistries of fractures and matrix to be treated separately. Since interaction between these continua is also considered, fracture-matrix chemical and mineralogical interaction can be represented and monitored. This methodology also allows

evaluation of the consequences of fracture and matrix transport on the mineralogical and chemical changes occurring along a flow pathway.

Chemically and mineralogically heterogeneous initial conditions and source terms.

The structure of the code allows an unlimited number of discrete chemical and mineralogical conditions to be represented. This heterogeneity can be spatial, thus allowing any configuration of mineralogically or chemically distinct systems to be represented, or it can be temporal, allowing time-varying chemical inputs to the system.

Time-varying rock and fracture permeability. Pore volume change reflects the effects of dissolution and precipitation. The functional relationship between porosity and permeability is treated as a cubic law along the lines of a Kozeny-Carmen relationship, but the code is capable of handling any functional relationship one chooses.

Parallelization of NUFT-C. The Message Passing Interface (MPI, 1995; MPI-2, 1997) standard protocols were implemented to facilitate parallel computations. This standard is supported on the ASCI machines and thus its use is intended to achieve maximum efficiency for parallel computations. In addition, the internal mesh generation capabilities of NUFT were expanded to allow global definition of cell attributes (chemical, mineralogical and physical properties, for example) in the input file, thus simplifying the initial descriptions of the data structure.

Implementation of PETSc. Numerical solution of the large sets of partial differential equations inherent in these calculations has been accomplished by use of the Portable, Extensible Toolkit for Scientific Computation (Balay et al., 1997). Although NUFT and NUFT-C can use other solver packages, PETSc was chosen for this application because of its extensive library of routines, and its high level of support on the ASCI machines.

Run-time monitoring and post-processing capabilities. A suite of routines was developed to allow visualization of both performance and simulation results while a simulation is running as well as after simulations are complete. These capabilities include graphics packages showing changes in specific solution components and mineral abundances, changes in temperature, saturation, gas fraction and pressure, time derivatives of the abundance of specified chemical components and minerals, changes in the magnitude of time steps as a function of number of time steps, and the simulated time versus the elapsed time.

Performance on the ASCI Blue Pacific IBM SP-2

Computational Phases

A typical coupled thermal-hydrological-geochemical calculation done using NUFT-C will consist of several different computational phases with different performance characteristics. These phases include local and global computational phases.

The local computational phases consist of calculations involving only the variables of one grid cell. Parallelization of these local calculations is straightforward and the performance of this phase is high. The calculations performed at each grid cell are identical, except for the number of variable switching iterations in the thermal-hydrology and chemistry models, so static load balancing by assigning an equal number of grid cells to each processor is generally effective.

The global computational phases consist primarily of the linear solver portion of the solution for the partial differential equations. This is the only phase involving extensive interprocessor communication. We used the parallel linear solver from the PETSc software package, modified by us to address specific needs arising from this coupled calculation

Performance Characteristics

The linear system which must be solved globally in the thermal-hydrology model is the most difficult calculation numerically. The system is not symmetric, not positive definite and very poorly conditioned. In a typical calculation in which heat is added to the system and the temperature changes, the thermal-hydrology conditions become more complex with multi-phase flow, possibly boiling, condensation and widely different flow velocities in different media. As a result the linear systems become more and more stiff. Through experimentation with the GMRES (and other) solvers with Additive Schwarz Method (ASM) preconditioning, a two-level multi-grid preconditioner, and a Multiplicative Schwarz Method (MSM) preconditioner, we established that the latter, with the GMRES linear solver, provides the best performance for this application. Even so, as the system becomes stiffer, time stepping is often reduced to seconds or minutes in a complex calculation.

Although the linear system in the thermal-hydrology model is the most difficult calculation, in a typical moderate size problem with complex chemistry, thermal-hydrology only accounts for a small percentage (<10%) of the run time. This results from the fact that the time scales involved in the chemistry model usually require the use of smaller time steps than the thermal-hydrology model, often by a factor of ten or more. Also, the local calculation phase of the chemistry model is far more complex than any other calculation phase and represents the bulk of the run time. There is (at least) one global linear system solution performed at each chemistry time step. These global systems are larger than the thermal-hydrology linear systems, but are far simpler numerically. It is not unusual for these linear systems to converge in one or two iterations using the simplest PETSc solvers and do not represent a significant part of the run time.

Global Performance

Because of schedule limitations, the current version of the code has not been tuned to improve the scalar performance on the 604e processors of the IBM SP-2 machine. This effort will be undertaken separately. The local phase of the chemistry model runs at 30 MFLOPS per processor for large numbers of chemical species per cell. With tuning, we believe this performance can be improved by better than a factor of 2. The global chemistry calculations also scale essentially linearly as the number of processors and the number of grid cells are increased, and will thus allow excellent performance. Thermal-hydrology calculations are less efficient. The difference in performance depends upon the specific calculations being done. This part of the calculation tends to be the performance limiting aspect of the code, and can be as low as 50% of the chemistry model.

IV. VALIDATION

Validation of the code was accomplished by comparing simulation results with those of another benchmark code (GIMRT, Steefel and Yabusaki, 1997; Steefel, 2000) that is useful for constant temperature, fully saturated systems. Comparison has also been made with bench scale experiments, field scale experiments, and field studies. Summarized here are the results of a few of those exercises.

Plug Flow Reactor Experiments

Well-constrained physical experiments are of paramount importance for conducting validation of codes designed to model reactive transport. However, there are no published experiments in which sufficient data collection and experimental control were achieved to rigorously test all capabilities of NUFT-C, including the chemical and mineralogical evolution of geological systems under both saturated and unsaturated, non-isothermal conditions. One set of saturated, isothermal experiments that does provide sufficient data to test the representation of mineral dissolution and precipitation is a suite of plug flow reactor studies (Johnson et al., 1998). In these experiments, tube-like titanium reactor vessels were carefully packed with quartz (experiment PFR-3) and tuff (experiment PFR-5) of known grain size and surface areas. The reactor vessels were placed in furnaces and maintained at constant temperature ($\sim 240^{\circ}\text{C}$) and fluid fluxes for times of 12.7 (PFR-3) to 36 (PFR-5) days. Fluid exiting the reactor was periodically sampled and analyzed (see Johnson et al., 1998 for detailed description of experimental conditions). These data provide a time history of reactive transport of water through the reactor, allowing comparison between measured and simulated dissolution histories for the simple chemical system SiO_2 (quartz only - PFR-3) and the complex chemical system Na-K-Ca-Al-Si-O (quartz-cristobalite-potassium feldspar-plagioclase plus secondary precipitates - PFR-5).

The method employed for the quartz dissolution experiment was to use the measured surface area of the crushed quartz and iteratively solve for the dissolution rate constant that provides the best match between measured and observed effluent aqueous SiO_2 concentration. This rate constant is then compared to the rate constant determined from independent laboratory measurements. As is clear from Figure 2, the correspondence between the deduced and measured rate constants for quartz dissolution is excellent.

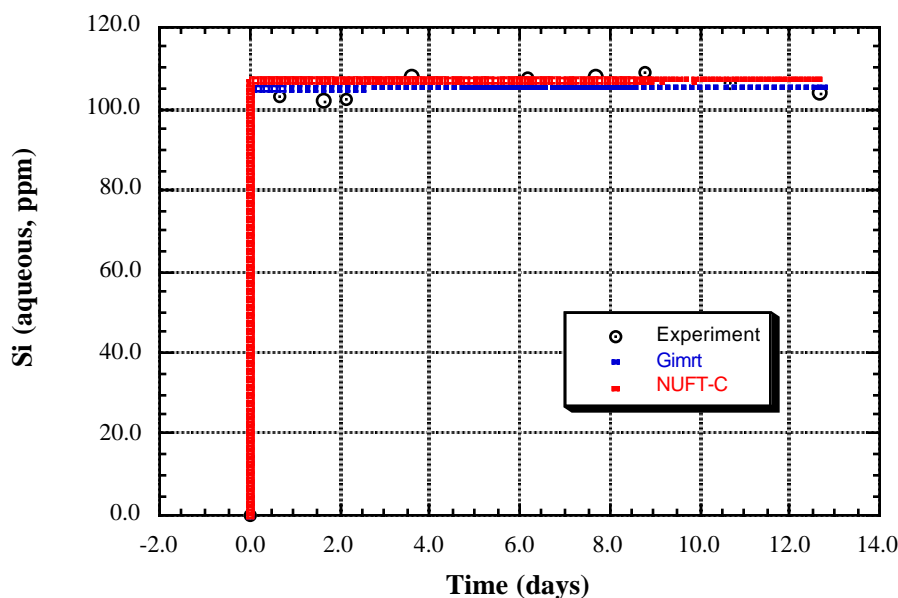


Figure 2: Dissolved silica concentration as a function of time for the PFR-3 experiment. For comparison, the results of the GIMRT (Steeffel, 2000) and NUFT-C simulations for this specific experiment are also shown.

The approach taken for the chemically more complex PFR-5 experiment was to use best estimates for the dissolution rate constants for the mineral phases initially present, and for the supersaturation thresholds for potential secondary mineral precipitates. Through a series of iterative steps, these variables were modified to achieve the best match between observed and simulated effluent chemical composition as a function of time. Although excellent matches for some chemical species can be obtained, discrepancies persist for both the benchmark code (GIMRT) and the new code (NUFT-C), despite numerous iterations using a range of values for the appropriate variables (Figures 3 and 4). In this case, the close correspondence between codes, and the contrasts with the measured values highlights the limitations of existing data and numerical models. The primary source for the discrepancies comes from the absence of well-constrained numerical models for precipitation kinetics (including representation of dynamic surface areas, controls on nucleation events, and rate dependence on saturation state) (Johnson et

al., 1998). Hence, in this instance, the validation exercise provides a demonstration that NUFT-C provides state-of-the-art capabilities, within the limitations of the existing experimental and scientific knowledge base.

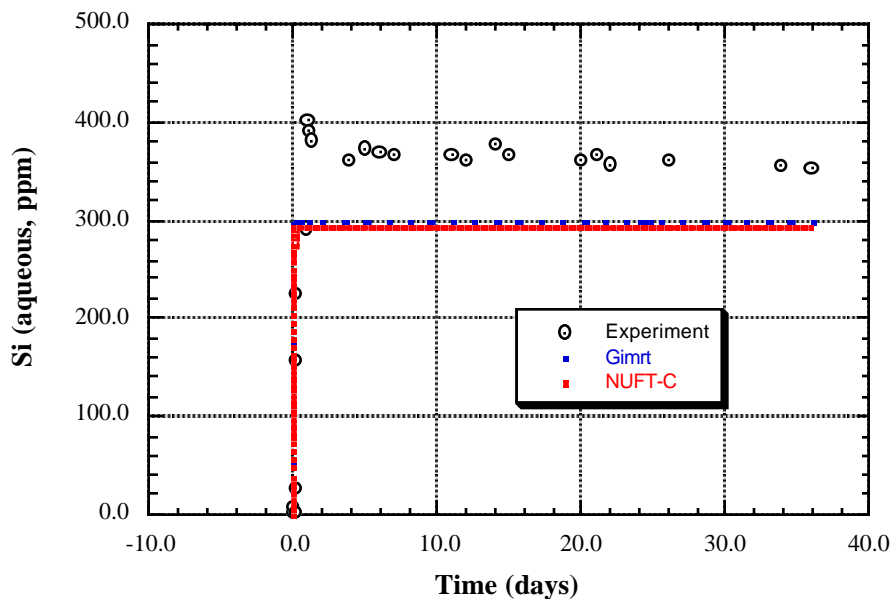


Figure 3: Dissolved silica concentration as a function of time for the PFR-5 (i.e., tuff) experiment. For comparison, the results of the GIMRT (Steefel and Yabusaki, 1996) and NUFT-C simulations for this specific experiment are also shown.

Drift-Scale Test

During the latter part of the 1990s the Yucca Mountain Project conducted a field scale test that provides data useful for testing certain aspects of gas-phase chemical changes during the course of heating rock under non-isothermal and unsaturated conditions. This test was conducted from December, 1998 through mid-2000. The test consists of a tunnel in which 47.5 meters of its length encloses 9 electrical resistance heaters. The tunnel is 4.42 meters in diameter and the heaters are 1.5 meters in diameter and ca. 5 meters long. The purpose of the test was to conduct a 0.7 scale experiment in the same geological material that would enclose an actual tunnel in which nuclear waste packages would be emplaced. The test was conducted to examine the response of the geological system to such a heat load. Measurements and sampling were done by means of a series of boreholes that were drilled above and below the heated area. Particularly important for this validation exercise were ca. 3 inch boreholes that were drilled perpendicular to the heated

tunnel from an adjacent tunnel. These boreholes were separated into segments of a few meters length by means of inflated “packers”. Gas samples were collected from the packed-off intervals and analyzed for CO₂ content (Figure 5) at irregular intervals. Although a very limited suite of water samples was also collected from some of these intervals, the sampling constraints on those samples are not sufficient to allow them to be used for rigorous code validation efforts.

Simulations were conducted using NUFT-C in order to compare predicted and measured CO₂ concentrations in the gas phase. These simulations were done using the rock property data produced by the Yucca Mountain Project for the rock materials surrounding the tunnel. It is also

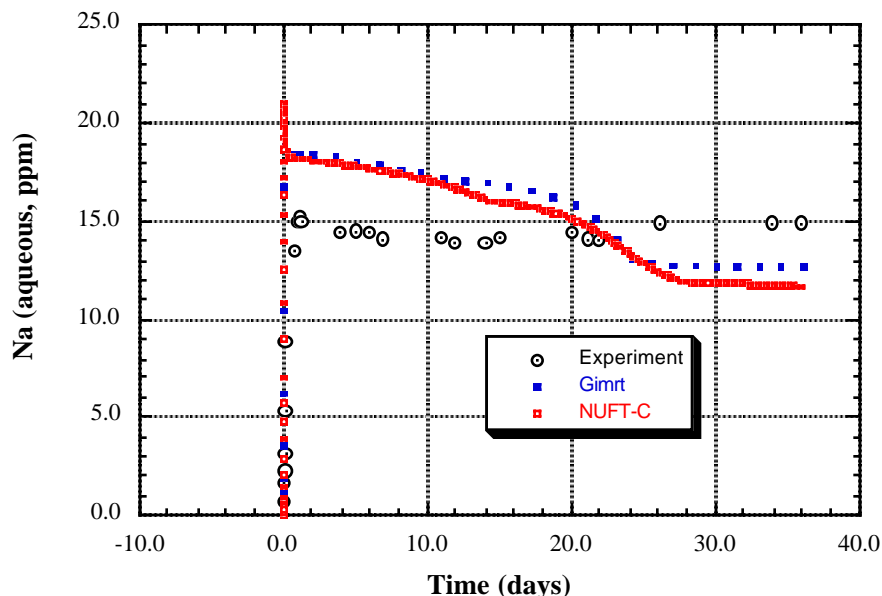


Figure 4: Dissolved sodium concentration as a function of time for the PFR-5 (i.e., tuff) experiment. For comparison, the results of the GIMRT (Steefel and Yabusaki, 1996) and NUFT-C simulations for this specific experiment are also shown.

important to emphasize that these simulations were conducted prior to any knowledge of the results of the gas measurements.

In this simulation the geometry and heat output of the heaters was taken into account. The simulation was done using the Yucca Mountain Project description of the thermal-hydrological properties of the rock and considered the system Ca-Si-O-CO₂. The results of the simulation, at 0.9 years, is shown 2-dimensionally in Figure 6. The CO₂ concentration (by volume) through the simulation domain along the lines equivalent to Boreholes 76 and 78 is shown in the line graphs of Figure 7 and 8 for comparison.

Although spatial resolution of the simulation is much finer than that for the field measurements, thus preventing direct one-to-one comparisons of CO₂ concentration as a function of location, the correspondence between measurements and simulation results is striking. For example, even though the field samples were not collected at sufficiently small enough spatial intervals to allow recognition of the dip in CO₂ concentration immediately over the drift, which separates regions of elevated CO₂, the measurements are consistent with the general pattern of significantly elevated CO₂ in areas above and to the sides, and immediately around the tunnel.

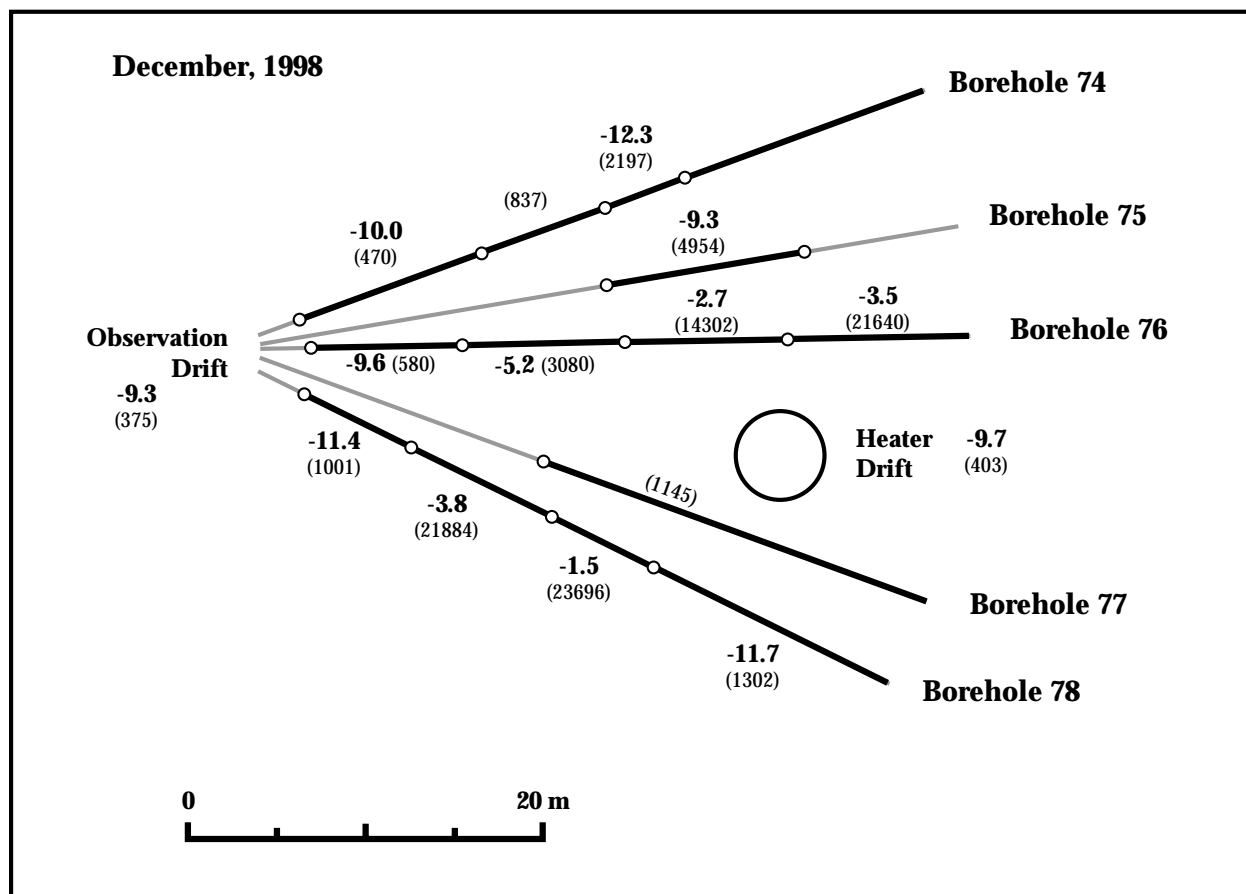
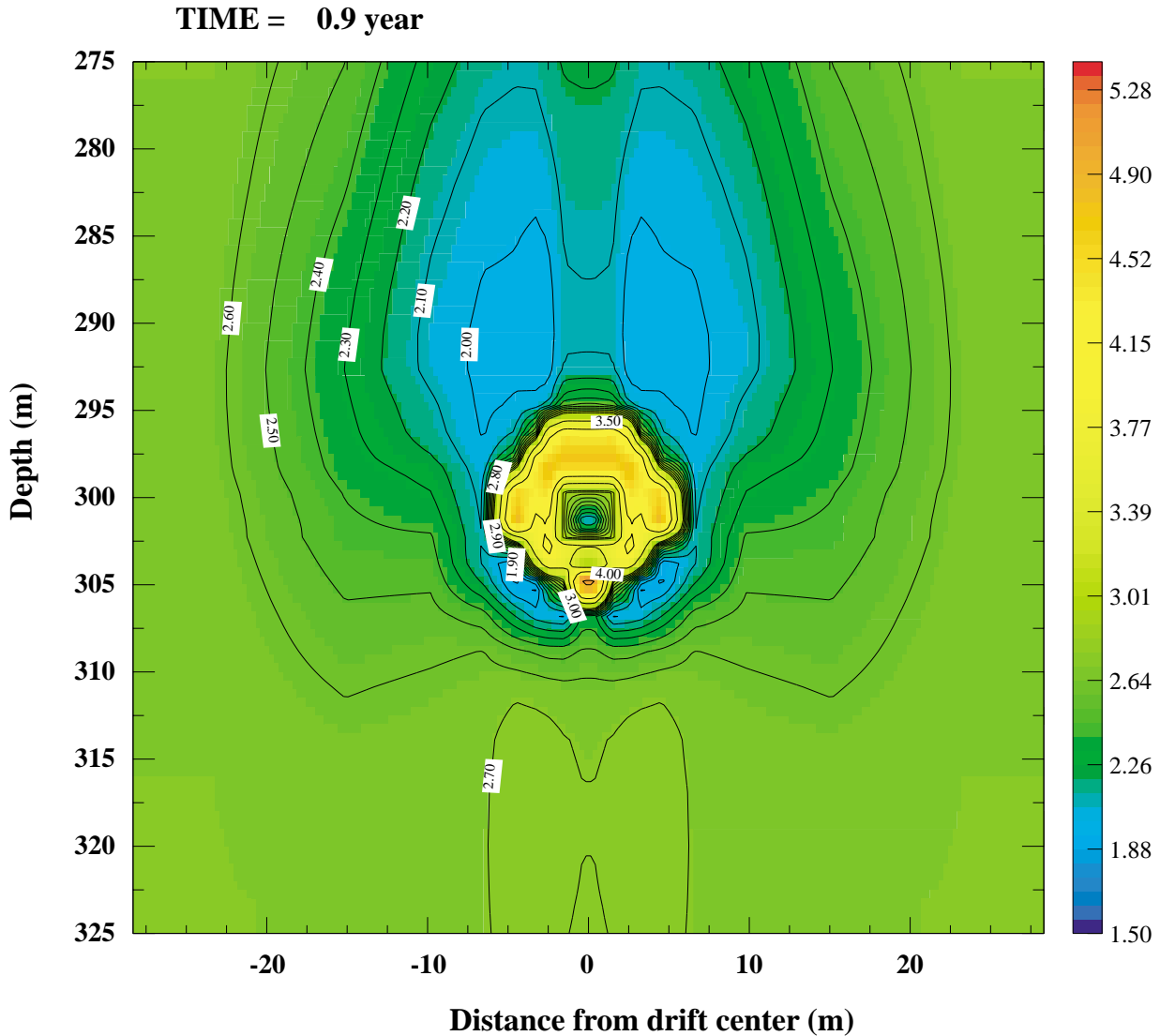


Figure 5. $\delta^{13}\text{C}$ data for CO₂ (in ‰ units relative to VPDB) in gas samples collected from boreholes 74-78 around the Heater Drift. Also given in parentheses are the concentrations of CO₂ (ppmv).

Also evident in the simulations is the rapid change of CO₂ locally. The simulations show that within 6 weeks, CO₂ concentrations could be expected to change by more than half a log unit in some locations. Hence, field measurements taken on a monthly or longer time scale, such as these were, will tend to smear out time variability, and thus make comparisons more difficult.

These results are significant for two reasons. First, they demonstrate the ability of this simulation tool to produce spatially and temporally accurate descriptions of gas phase composition in a thermally, hydrologically and structurally complex setting. Second, these

simulations demonstrate the benefit that could be achieved using a tool like this to guide sampling strategies in field testing and monitoring programs. Specifically, had these simulations been available prior to the testing program, it would have been immediately apparent where and on what spatial and temporal scales sampling should be done. Coordinating simulation results and sampling programs can enhance confidence in models, understanding of physical processes and simulation accuracy.



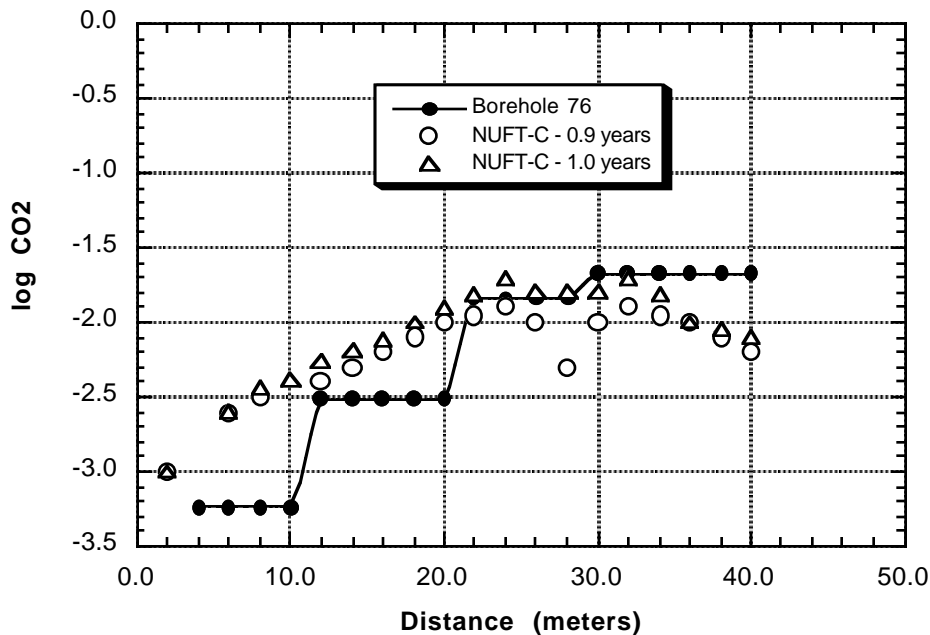


Figure 7: Comparison between measured CO₂ gas phase concentrations along borehole 76 (Figure 5), and NUFT-C simulations (open symbols; see Figure 6 for full 2-D representation of gas-phase CO₂ at 0.9 years). Note that the horizontally grouped filled circles do not represent individual analyses but, rather, the distance ranges over which a specific log CO₂ measured value applies. The results of simulations at 0.9 years and 1.0 years are shown to demonstrate the dynamic nature of this system.

Yucca Mountain Pore Waters

The Yucca Mountain Project has drilled numerous wells to obtain data for site characterization. One such well (UZ-14) was drilled with the express purpose of gaining information about hydrological properties and pore water compositions for the rock units that compose the region. The resulting water compositions (Yang et al., 1996, 1998) were later re-evaluated to address issues raised concerning the analyses (Browning et al., 2000). These data provide an exceptional opportunity to conduct a code validation exercise. Conceptually, the pore water in the natural system must reflect, to some degree, the result of infiltrating rainwater chemically interacting with each individual rock unit as it percolates from the ground surface to the water table. Hence, the extracted pore water compositions should reflect the progression of this water-rock interaction.

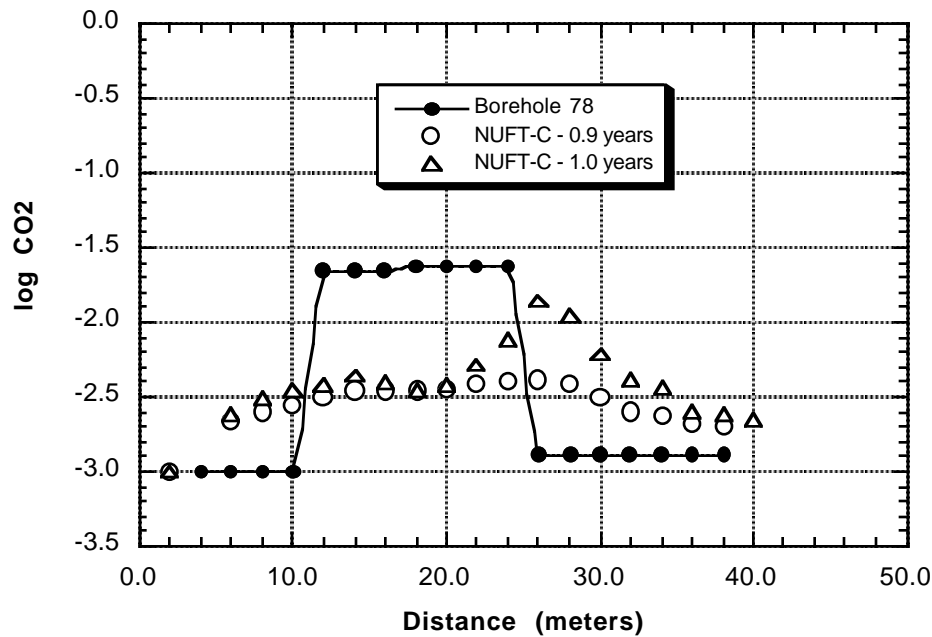


Figure 8. Comparison between measured CO_2 gas phase concentrations along borehole 78 (Figure 5), and NUFT-C simulations (open symbols; see Figure 6 for full 2-D representation of gas-phase CO_2 at 0.9 years). Note that the horizontally grouped filled circles do not represent individual analyses but, rather, the distance ranges over which a specific $\log \text{CO}_2$ measured value applies. The results of simulations at 0.9 years and 1.0 years are shown to demonstrate the dynamic nature of this system.

We conducted a series of simulations using NUFT-C in order to evaluate the ability of the code to reproduce the observed water compositions. We utilized the conceptual model of water-rock interaction resulting from rain water infiltration and percolation described above. The rock units and their respective thermal, hydrological and mineralogical properties were those utilized in other Yucca Mountain Project studies (YM Document MDL-NBS-HS-000001). These simulations included the simplifying assumptions employed in that report, namely a reduced suite of minerals to represent the rocks, and slower dissolution rates for calcite and glass than have been experimentally observed. We also conducted simulations using those same thermal and hydrological properties, but with a more robust suite of minerals, fewer rock units (to examine extent to which detailed stratigraphy is needed to accomplish code validation), and utilizing the laboratory measured (i.e., faster) dissolution rates. Below we discuss only a selection of those results, for the sake of brevity.

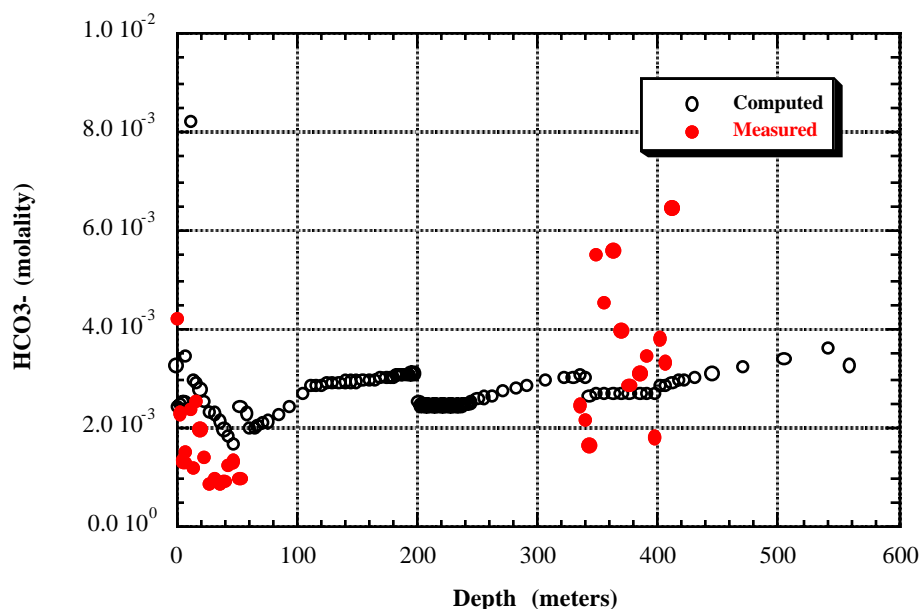


Figure 9. Computed HCO_3^- concentration as a function of depth, using the simplified chemical system, compared to pore water compositions measured from samples from borehole UZ-14. The pore water compositions are those reported by Browning et al., 2000.

Success at matching the observed water compositions varies due to differences in available data on rock properties. Within the upper ca. 100 meters of the section thermal-hydrological-mineralogical units are characterized on the scale of tens of meters, thus providing relatively high spatial resolution for the properties of the rock units. Between ca. 100 and 300 meters depth no data are available on water chemistry because water extraction from those units was not successful. At depths greater than ca. 320 meters, and down to approximately 600 meters, water analyses are available but only 4 rock units were characterized throughout this interval, thus providing relatively coarse spatial resolution for the thermal-hydrological-mineralogical rock properties.

Comparison between simulated and observed water compositions for both the simplified (Figures 9-11) and complex (Figures 12-15) systems is excellent within the shallower depth interval. Both the general trend of compositional change with depth, and the absolute abundances match well. At the deeper depth interval, the observed and simulated results approximately correspond, although the absence of detailed stratigraphy precludes achieving a better match.

For the simulations using the more robust chemical system, the match achieved between observed and simulated water compositions is of similar accuracy as that for the simplified system, but also extends to the other elements. As well, the results emphasize again the importance of obtaining spatially detailed characterization of the rock units, in order to achieve a high correspondence between measured and simulated water compositions.

In summary, utilizing a wide range of systems against which to compare simulation results, we have been able to validate NUFT-C for coupled thermal-hydrological-geochemical simulations for isothermal and non-isothermal, saturated and unsaturated

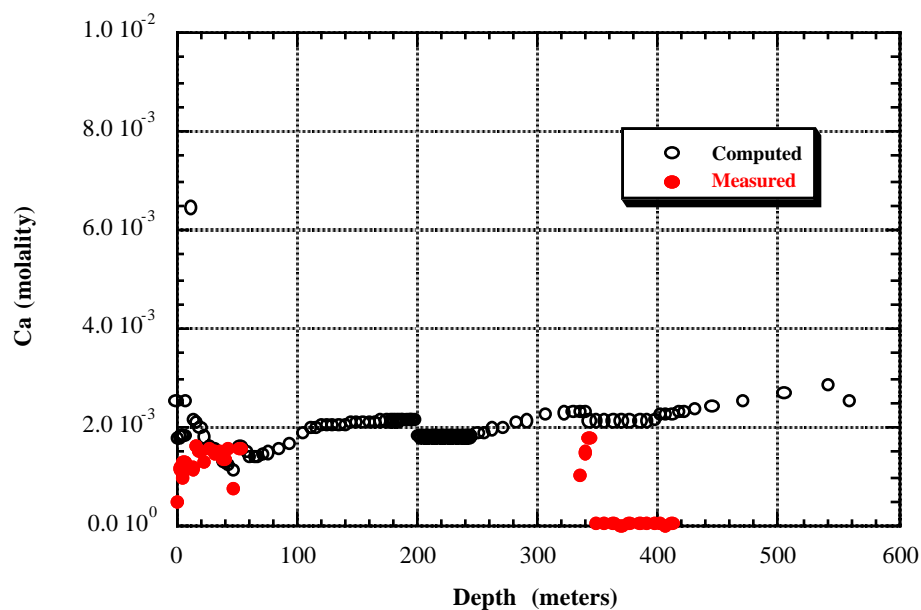


Figure 10. Computed Ca concentration as a function of depth, using the simplified chemical system, compared to pore water compositions measured from samples from borehole UZ-14. The pore water compositions are those reported by Browning et al., 2000.

conditions using simple and complex chemical systems. These validation exercises have been accomplished using data directly reported from laboratory and field experiments and observations. These results demonstrate that NUFT-C provides realistic representation of coupled thermal-hydrological-geochemical processes. The primary limitation to its ability to represent such processes lies in limitations for the data that characterize the system being considered.

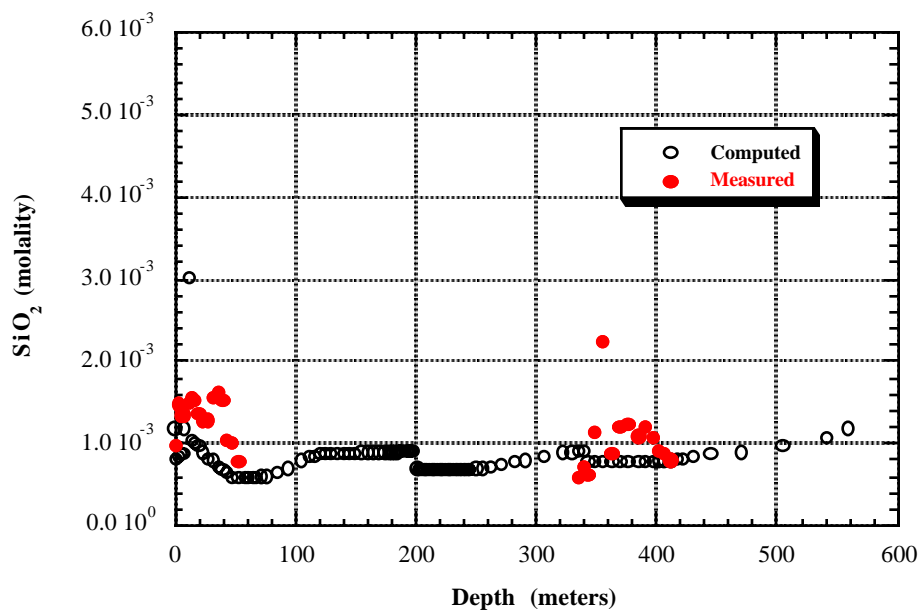


Figure 11 Computed dissolved silica concentration as a function of depth, using the simplified chemical system, compared to pore water compositions measured from samples from borehole UZ-14. The pore water compositions are those reported by Browning et al., 2000.

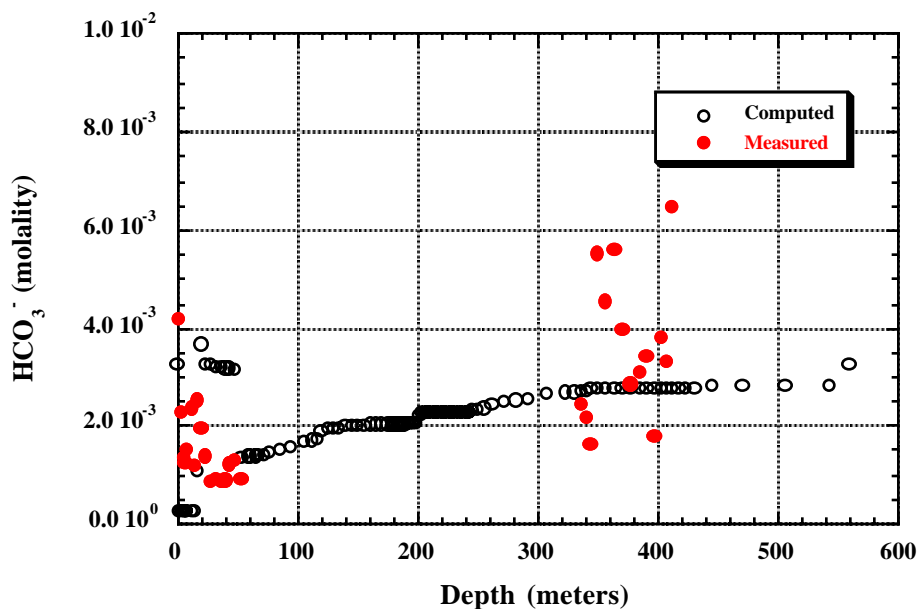


Figure 12. Computed dissolved bicarbonate concentration as a function of depth, using the complex chemical system, compared to pore water compositions measured from samples from borehole UZ-14. The pore water compositions are those reported by Browning et al., 2000.

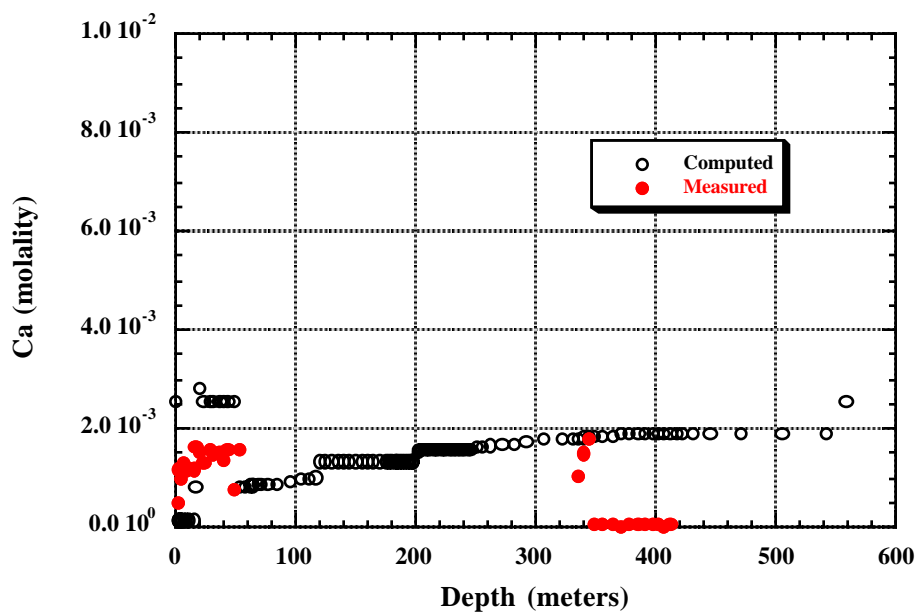


Figure 13. Computed Ca concentration as a function of depth, using the complex chemical system, compared to pore water compositions measured from samples from borehole UZ-14. The pore water compositions are those reported by Browning et al., 2000.

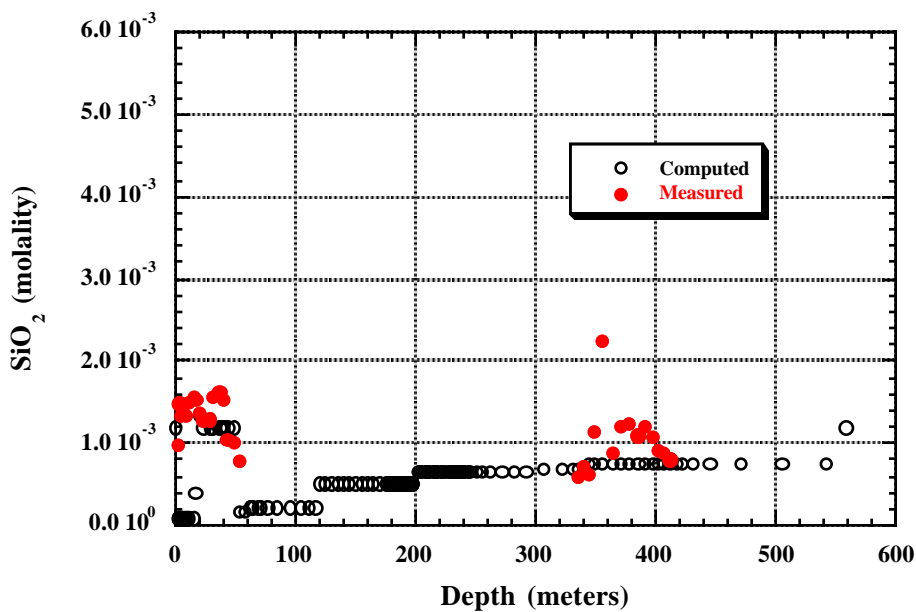


Figure 14. Computed aqueous silica concentration as a function of depth, using the complex chemical system, compared to pore water compositions measured from samples from borehole UZ-14. The pore water compositions are those reported by Browning et al., 2000.

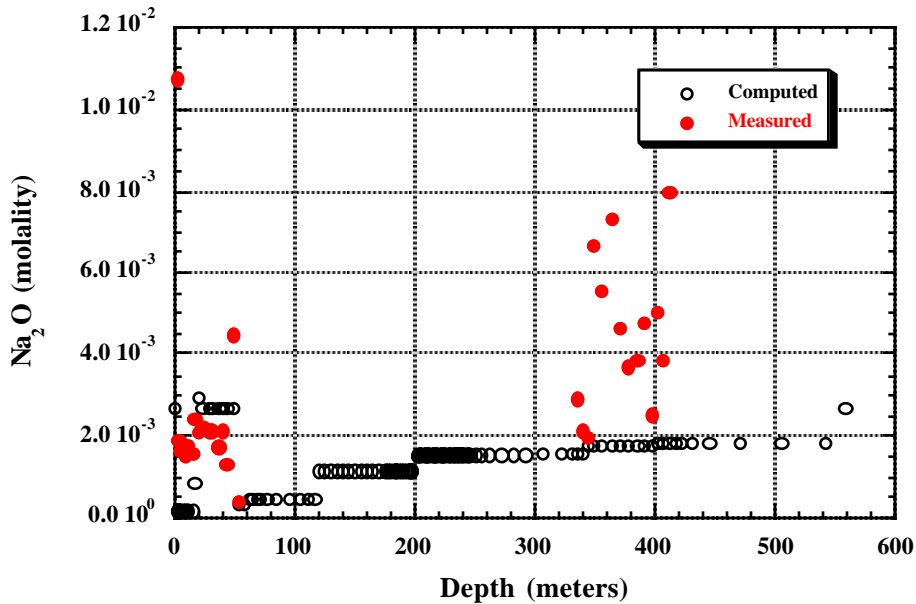


Figure 15. Computed dissolved sodium concentration as a function of depth, using the complex chemical system, compared to pore water compositions measured from samples from borehole UZ-14. The pore water compositions are those reported by Browning et al., 2000.

V. TECHNICAL OUTCOME

Applications to a Potential High Level Nuclear Waste Repository

The primary purpose of this Strategic Initiative was to develop a new research tool that would provide the ability to answer questions regarding the thermal-hydrological-geochemical evolution of high level nuclear waste repositories that could be answered through the application of massively parallel high performance computational platforms. The goals of providing this capability are to reduce reliance on model abstractions, represent more rigorously the processes that affect repository evolution, facilitate design and execution of monitoring programs, and enhance confidence in projected performance. To this end, NUFT-C was exercised in several different applications that considered certain key aspects of the response of the natural system to waste emplacement. Many of these simulations represent the first time such calculations have been completed on such a large and complex geological system at high resolution. These simulations ranged in size from two waste emplacement tunnels containing a total of twenty individual waste containers, to very large simulations that considered 100 waste containers distributed throughout five tunnels. In these the chemical system consisted of the primary

species, secondary aqueous species, and mineral phases listed in Table 1. The independent variables in the chemical and mineralogical system totaled 46 (primary aqueous species plus all considered mineral phases). The total number of independent hydrological properties considered exceeded 45 per each rock unit, of which there was a minimum of eight. The number of processors used in the simulations varied, depending upon the size of the computational mesh, and ranged between ca. 20 to 480 processors.

Many of these simulations examined the magnitude and extent of modification of rock properties, and the related chemical evolution associated with these changes, that might be expected at the extreme corner of a repository where thermal gradients may be most profound. Also considered were questions regarding the nature and extent of chemical changes that might be possible to monitor during a “performance confirmation” effort that would measure changes for the first 100 years of repository operation. Described below are important results from those simulations.

Table 1. Primary and secondary aqueous chemical species, and primary and secondary mineral phases used in the simulations.

Aqueous Species		Mineral Species	
H ⁺	primary	Albite	primary
Ca ⁺⁺	primary	Anorthite	primary
K ⁺	primary	Calcite	primary
Na ⁺	primary	Clinoptilolite-Ca	primary
Mg ⁺⁺	primary	Clinoptilolite-Na	primary
SiO ₂	primary	Cristobalite	primary
Al ⁺⁺⁺	primary	Glass	primary
HCO ₃ ⁻	primary	K-Feldspar	primary
Cl ⁻	primary	Montmorillonite	primary
SO ₄ ⁻	primary	Quartz	primary
O _{2-g}	primary	Amorphous SiO ₂	primary
tracer	primary		
OH ⁻	secondary	Analcime	secondary
AlO ₂ ⁻	secondary	Boehmite	secondary
AlO ⁺	secondary	Chalcedony	secondary
AlOH ⁺⁺	secondary	Clinochlore	secondary
HalO _{2-aq}	secondary	Dolomite	secondary
CaHSiO ₃ ⁺	secondary	Gibbsite	secondary
CaOH ⁺	secondary	Gypsum	secondary
CaCl ⁺	secondary	Halite	secondary
CaCl _{2-aq}	secondary	Heulandite-Ca	secondary
CaHCO ₃ ⁺	secondary	Heulandite-Na	secondary
CaHSiO ₃ ⁺	secondary	Hydromagnesite	secondary
CaCO _{3-aq}	secondary	Kaolinite	secondary
CaSO _{4-aq}	secondary	Laumontite	secondary
ClO ⁻	secondary	Mordenite-Ca	secondary
ClO ₂ ⁻	secondary	Mordenite-Na	secondary

ClO_3^-	secondary	Natrolite	secondary
ClO_4^-	secondary	Paragonite	secondary
$\text{HClO}_4\text{_{aq}}$	secondary	Pyrophyllite	secondary
$\text{HClO}_2\text{_{aq}}$	secondary	Scolecite	secondary
CO_3^{--}	secondary	Sepiolite	secondary
$\text{CO}_2\text{_{aq}}$	secondary	Sylvite	secondary
$\text{CO}_2\text{_{g}}$	secondary	Talc	secondary
$\text{KCl_{aq}}$	secondary	Wairikite	secondary
$\text{HCl_{aq}}$	secondary		
$\text{KOH_{aq}}$	secondary		
$\text{KHSO}_4\text{_{aq}}$	secondary		
KSO_4^-	secondary		
MgHCO_3^+	secondary		
MgCl^+	secondary		
MgOH^+	secondary		
MgHSiO_3^+	secondary		
$\text{MgCO}_3\text{_{aq}}$	secondary		
$\text{MgSO}_4\text{_{aq}}$	secondary		
$\text{NaCl_{aq}}$	secondary		
$\text{NaOH_{aq}}$	secondary		
$\text{NaHSiO}_3\text{_{aq}}$	secondary		
NaSO_4^-	secondary		
$\text{O}_2\text{_{aq}}$	secondary		
HSiO_3^-	secondary		
HSO_4^-	secondary		
HS^-	secondary		
S_2^{--}	secondary		
S_2O_3^-	secondary		
SO_3^{--}	secondary		
$\text{H}_2\text{S_{aq}}$	secondary		
$\text{SO}_2\text{_{aq}}$	secondary		

Chemical and physical processes important for long term performance

Simulations done to consider long-term physical and chemical changes examined conditions at an external corner of a potential repository. This location was chosen the thermal gradients within the host rock would be at their most extreme. This environment was selected because it is likely that some of the important interactions that could take place in a potential repository would be in regions where thermal gradients are greatest.

For the case discussed here, the terminal ends of 2 tunnels were considered at the extreme edge of a potential repository. For this geometry number of simulations were carried out using

different numbers of waste packages (between 6 and 60), the difference reflecting the resolution required for the process under consideration. In the following discussion, we will focus attention on the effects of processes in the rock between tunnels, and on alteration that takes place at the ends of the tunnels.

One topic of interest is the extent to which interaction between waste emplacement tunnels would result in significant modification of the host rock between the tunnels. This issue is important because modification of hydrological properties of rock composing the so-called “pillar” regions between tunnels will influence the extent to which drainage of water can freely take place. Unimpeded water drainage through this “pillar” region will diminish the possible flux of water that could enter a waste emplacement tunnel, while plugging of pores and fractures in this region has the potential to increase water flux in the vicinity of the waste emplacement tunnels.

Simulations to consider this problem were done for simple chemical systems in which only silica was considered and thermal loads were extremely high, as well as more complex systems (Table 1) in which lower thermal loads, which are closer to those being considered for the Yucca Mountain Project, were used.

These simulations indicate that the primary mineral phases responsible for changes in porosity (and, hence, permeability) are clay minerals, silica polymorphs and calcite. In Figure 16 the abundance of calcite is shown, since it provides a good illustration of the complexities associated with this deposition process. This profile is taken along a line that runs perpendicularly through the tunnels, at an elevation about half way up the tunnel wall. The greatest volume of calcite is deposited within a few meters of the tunnel walls, reflecting the combined effects of elevated temperature, water evaporation, and rock water interaction. Because these simulations were done assuming that backfill would be present in the tunnels, calcite deposition also occurs there. Calcite abundance drops to zero in the region where slightly lower temperatures occur and water drainage is concentrated. Within the pillar regions, calcite abundance is approximately constant at about 5 parts per million, by volume.

The variable that most directly represents the combined changes in hydrological conditions due to mineral dissolution or precipitation is the ratio of initial to final porosity (“porosity ratio change”). In Figure 17 the regions of significant (greater than 0.1 volume percent absolute change) porosity increase and reduction are shown enclosed by the purple surfaces.

The regions of porosity increase tend to be concentrated above the tunnels, where refluxing of water occurs for a brief period during the heating phase of the simulation. These regions are approximately three meters thick. Immediately below these regions, adjacent to the crown of the tunnel, and also in the vicinity of the lower portions of the outer tunnel walls, are those regions where porosity reduction is most significant. Two distinct processes are responsible for these changes. Above

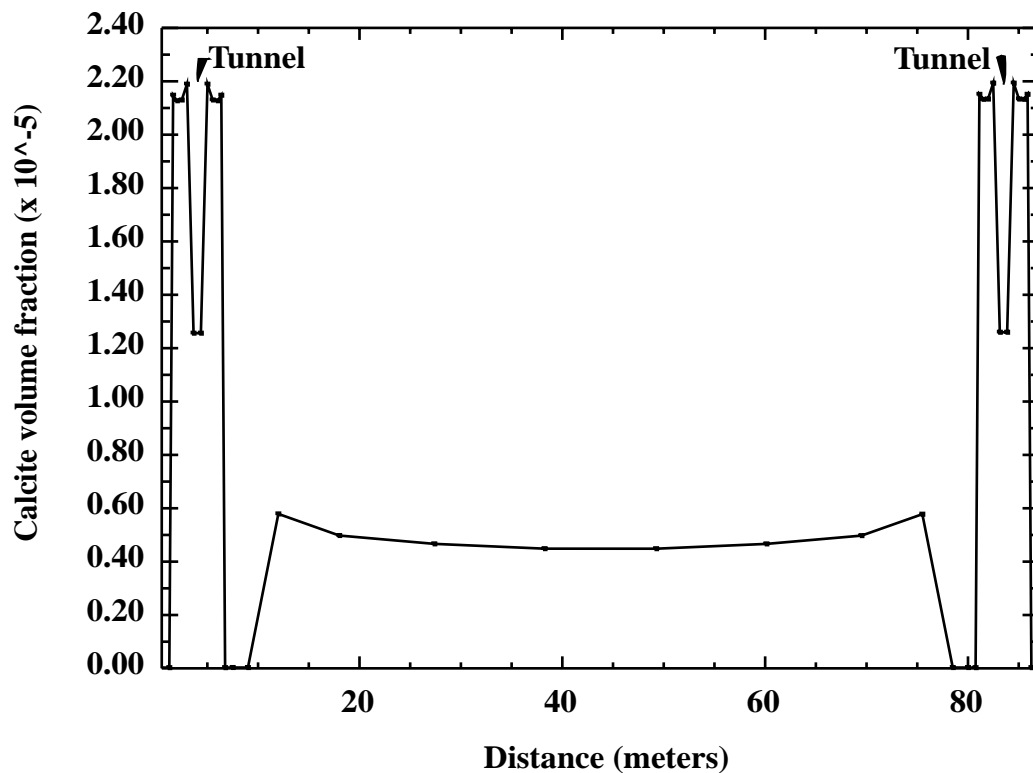


Figure 16. Volume fraction of calcite deposited between two waste emplacement tunnels, after 300 years. Note that the bulk of the calcite is deposited within a few meters of the tunnel edge, while the amount within the pillar region is less than 10 parts per million, by volume.

the tunnel, the refluxing process brings dilute solutions into areas where evaporation and boiling occur, resulting in precipitation of the small dissolved load carried by the evaporating and boiling water. In the vicinity of the lower portion of the tunnel walls, precipitation of minerals occurs because water draining from above this region passes through a zone of higher temperature before it begins to cool in this lower area. As cooling occurs, those minerals that are close to being saturated (primarily clays) at higher temperatures become supersaturated and precipitate.

Also shown in Figure 17 is the distribution of NaCl deposited in fractures. Salt deposition is restricted to those regions where complete or nearly complete drying occurred during the heating phase in this simulation. The maximum salt volume deposited is less than 10 parts per million. These results show two important features. First, nearly all salt deposition is limited to the areas along the sides of the tunnels, and very little is deposited in the rock immediately above the tunnel crown. This is important because salt that is dissolved as water returns toward the tunnels at later times will tend to be carried away from the tunnels as water flows along fractures past the tunnels. On the other hand, water entering the tunnels from above, in the vicinity of the crown, will have little salt available for dissolution and transport into the tunnel. This is significant for consideration of corrosion effects, and suggests that the bulk of the salts that might form during heating of the repository will likely have little opportunity to contact waste containers.

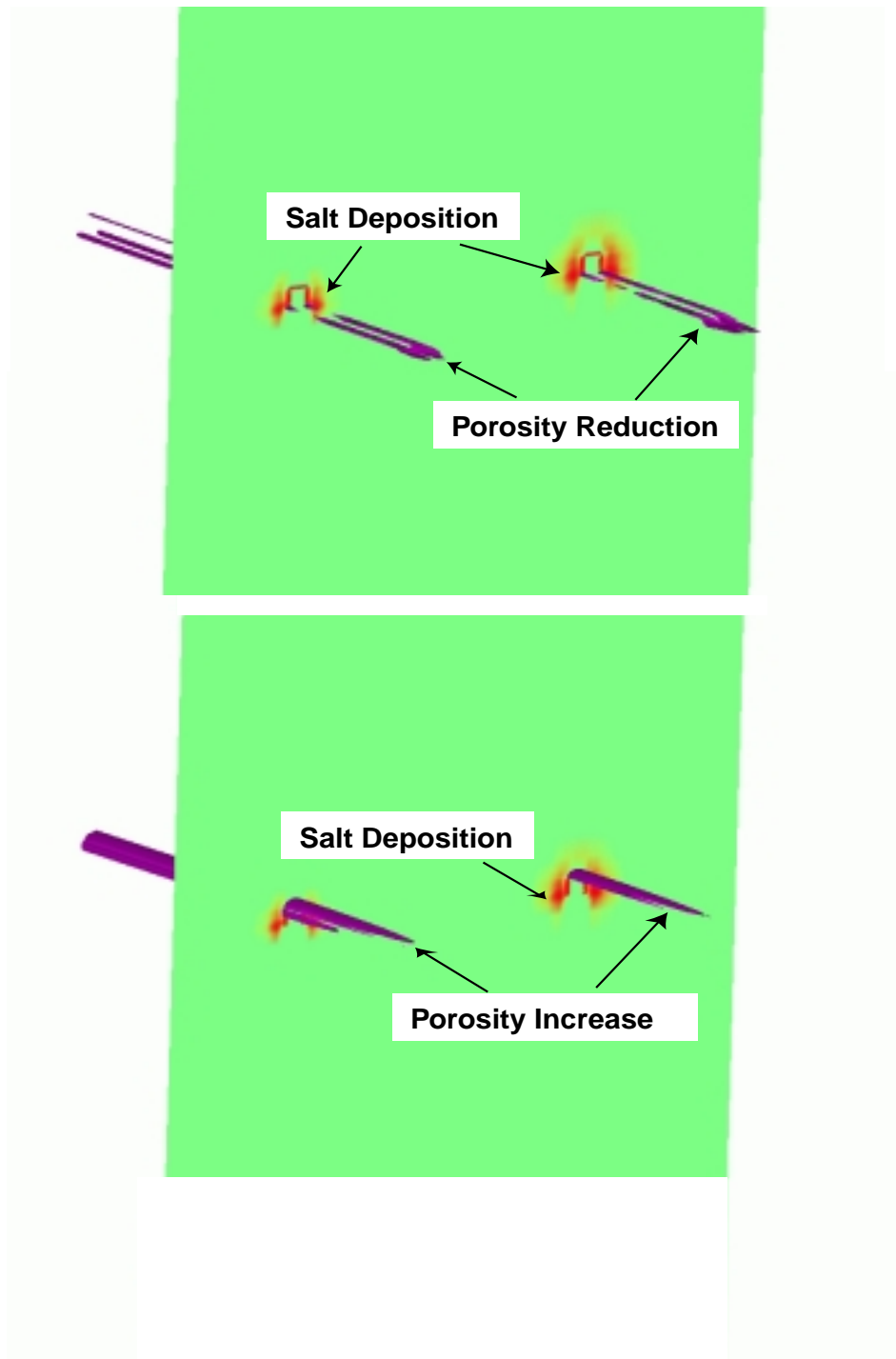


Figure 17. This 3-dimensional depiction shows the change in porosity and the location of salt deposition in fractures after the thermal maximum has been reached (300 years). The upper portion of the figure shows a two dimensional slice (green field) in which the regions of salt deposition (red haloes) are indicated. The tunnels themselves show up on the green fields as the solid red circles. In 3 dimensions, the tunnels would project toward the right and out of the page. Also shown in the upper panel is the 3-dimensional projection of the regions where porosity has been reduced by more than 0.1% (enclosed by purple surfaces). The lower panel is identical to the upper, except that the region of porosity increase, rather than reduction, is shown.

The other important point these simulations illustrate is that the unique thermal-hydrological environment of each waste emplacement tunnel will influence the extent and nature of mineralogical changes. Note, for example, that the region of porosity reduction is greatest near the ends of the tunnels, reflecting the effect of steep thermal gradients in those regions. Note also that the form of these regions of porosity change are similar, but not identical for the two tunnels. This reflects the local differences in heat and its impact on fluid movement, and provides an indication of the sensitivity of the system to heterogeneity imposed by engineering activities.

In summary, large scale simulations of the thermal-hydrological-geochemical evolution of a high level nuclear waste repository can provide important insights into the magnitude and nature of physical and chemical changes that might influence the overall performance of the repository. These insights provide a much deeper understanding of the actual distribution of a variety of effects that will be expressed in such an engineered facility, and can contribute to a greater degree of confidence that the performance of a repository can be evaluated.

Chemical and physical processes important for post-closure monitoring

Simulations of long-term (i.e., tens of years to thousands of years) performance of any geological repository for any material or waste can never be experimentally verified. The primary means for gaining confidence in the accuracy of simulated behavior is through comparing the predicted response of an engineered facility early in its performance period to measurements in that same facility for the same time period. Differences between simulated and measured results provide an opportunity to quantitatively evaluate uncertainties in predicted results. However, conducting such a testing program requires knowledge of what variables can be measured, what their values should be in specific locations, and how their values will change with time.

To provide insight into the variables that could be measured in a field program over a typical monitoring period (100 years), we conducted a series of simulations to examine in detail the measurability of chemical parameters. These simulations were done in three dimensions with twenty waste packages in a 2 emplacement tunnel model. Two types of waste packages were considered to be randomly distributed in the tunnels, with heat output between packages differing by 33%.

The simulations were done utilizing the dual porosity – dual permeability capability that allows representation of both fracture and matrix properties. The chemical system and mineral suite used in the simulations is that shown in Table 1. The results show several features that are important for design and execution of a performance evaluation program. Most striking is the clear indication that chemical variability through time is minimal for nearly all locations above the tunnels. In contrast, the greatest degree of chemical variability is located in those regions to the sides and below the tunnels. The reason for this pattern is that the pore water that evaporates and/or boils in the immediate vicinity of the tunnels travels a relatively short distance (a few meters to a few tens of meters) before it condenses. Once it condenses, it flows downward under the influence of gravity, draining away from the tunnels. The simulations demonstrate that most of this drainage flow is next to the tunnels. There is also a counter flow of pore gases upward

from below the tunnels and in the regions where drainage is occurring. This combination of flow patterns leads to complex chemical variability below the tunnels, despite the near absence of measurable change above the tunnels.

Parallel to the long axis of the tunnels some compositional variability (Figure 18) develops due to the effect of the different thermal outputs of the waste packages. However, the magnitude of the chemical contrasts along this trend and for this time period is not large and probably not measurable. Hence, the most advantageous regions for measuring chemical properties that could be useful for a monitoring program are located below the tunnels.

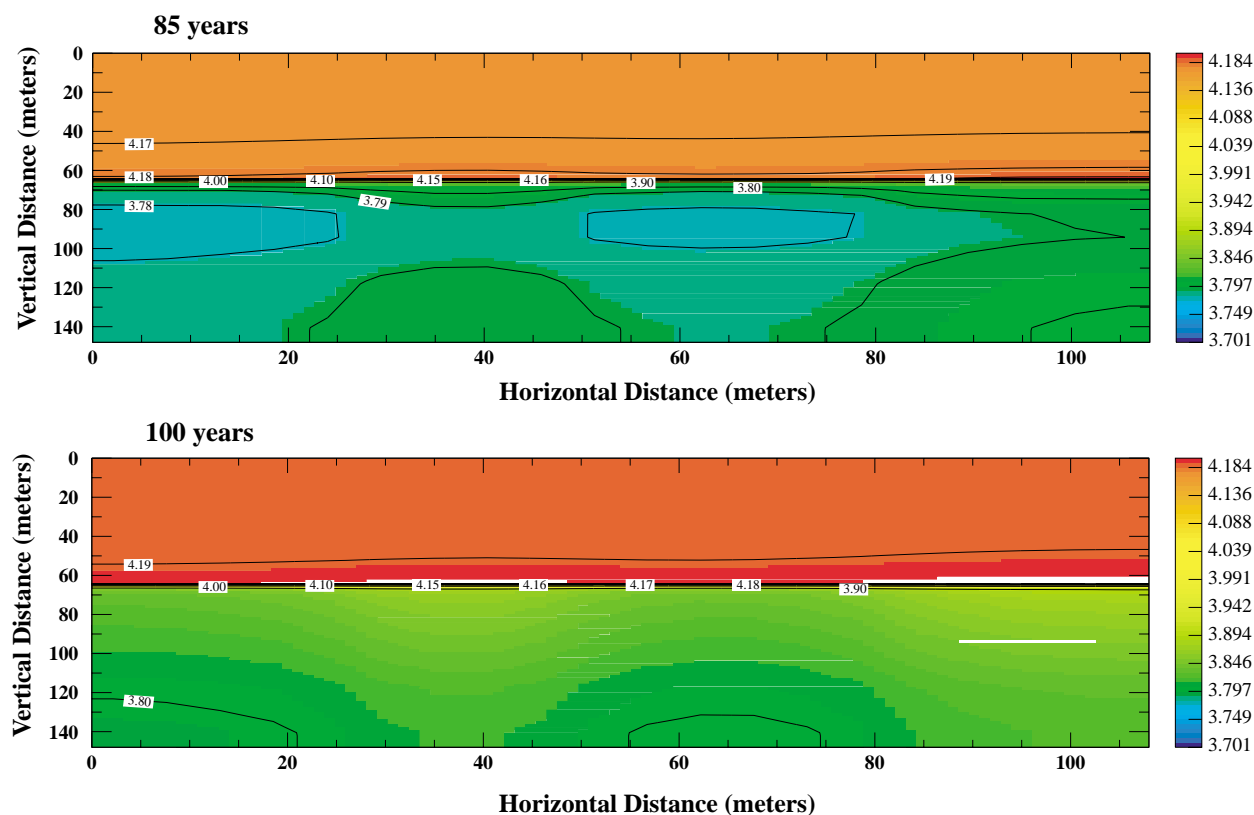


Figure 18. Sulfate concentration in fracture water along a plane parallel to, and 1 meter from a waste emplacement tunnel. Five of 20 waste packages are located within this representation of the system.

In addition, these simulations show that care must be exercised when developing a sampling program for a monitoring and performance confirmation activity. Some chemical species that are easily measured do not change sufficiently to be useful targets for monitoring. Other chemical species, however, change sufficiently over a 5 to 10 year time frame to allow implementation of a testing program that would evaluate both the absolute abundance of a chemical species as well as its time-dependent evolution. Both of these attributes of the chemical system (absolute abundance and rate of change) are important for assessing the accuracy of the projections developed on the basis of complex simulations. Calcium for example, is a chemical

constituent which is easy to measure in water samples, and which is important for understanding calcium carbonate formation. However, the changes in calcium concentration over time (Figure 19), and its degree of variability in space, are very small and would be a poor target for a measurement program.

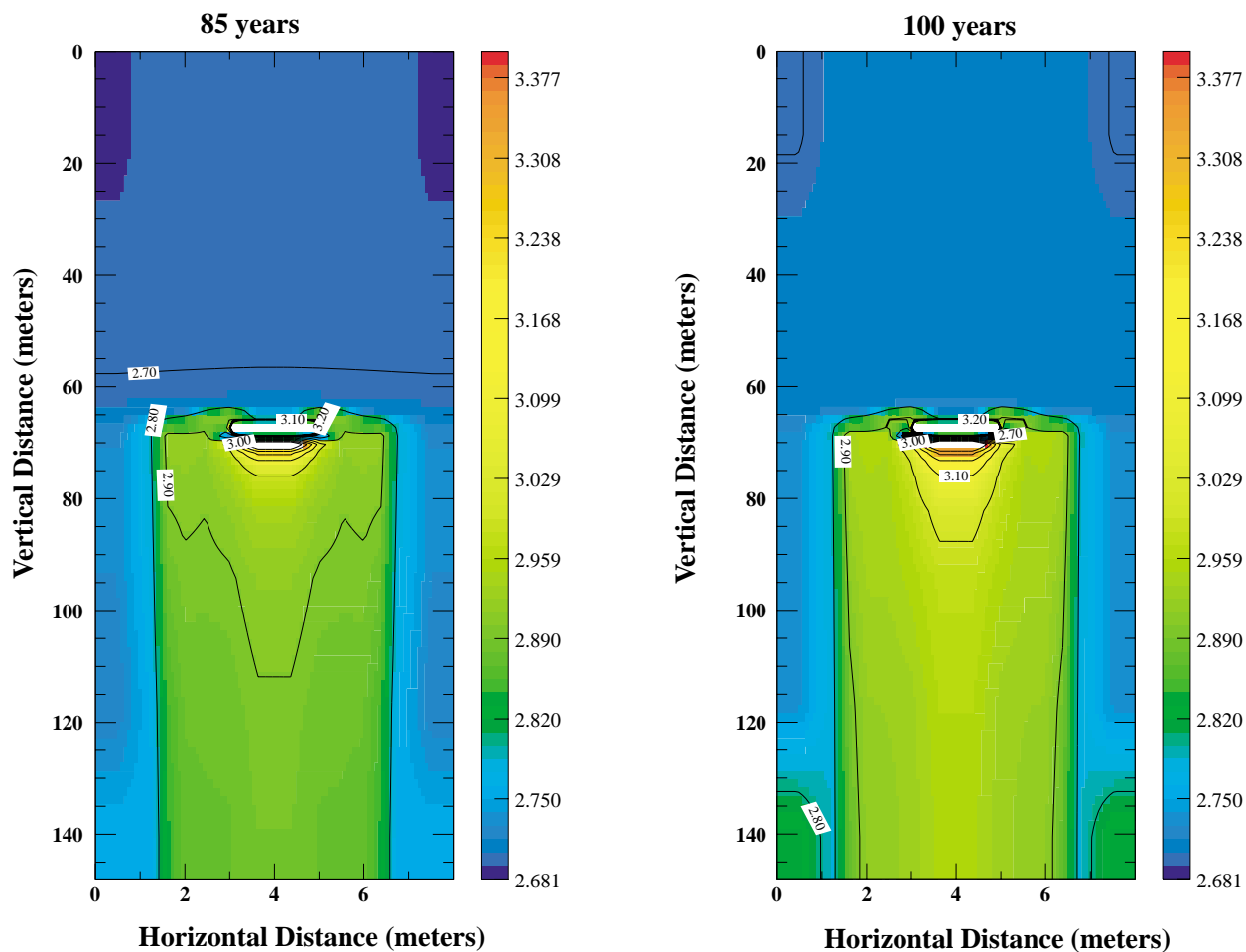


Figure 19. Cross section through a waste emplacement tunnel showing the concentration of calcium in fracture water at 85 years and 100 years after heating has begun. This cross section represents conditions 65 meters along the x-axis of Figure 18. The color bar scale is the same for both times and is the negative log of the concentration, in units of molality. Note the expanded horizontal scale that results in distortion of the tunnel shape. In the original simulations the tunnel was represented as a finely-meshed square opening. The distortion apparent in this figure is also present in Figures 20-22.

Bicarbonate (HCO_3^-), on the other hand, exhibits detectable spatial and temporal variability (Figure 20). Bicarbonate is useful to monitor because it, too, can be correlated with carbonate evolution. In addition, its abundance has an important influence on solution acidity and is responsive to changes in gas-phase CO_2 movement. Although bicarbonate measurement in the

field is challenging, it is a tractable problem and would be a reasonable target for a monitoring program. Monitoring CO_2 , in concert with HCO_3^- , adds valuable information that allows distinction to be made between the roles of carbonate and gas-phase CO_2 in controlling HCO_3^- . As noted previously in the discussion of code validation using the CO_2 data from the Yucca Mountain Drift-Scale Test, and as is evident from these simulations (Figure 21), such measurements must be done with sufficient spatial resolution to allow testing of model results. Similar arguments apply for the measurement of $\text{SO}_4^{=}$ (Figures 22), which plays an important role in the sulfide-sulfate system. The latter is important for considerations of system redox conditions, including the stability of sulfite which is a potential player in corrosion mechanisms and processes.

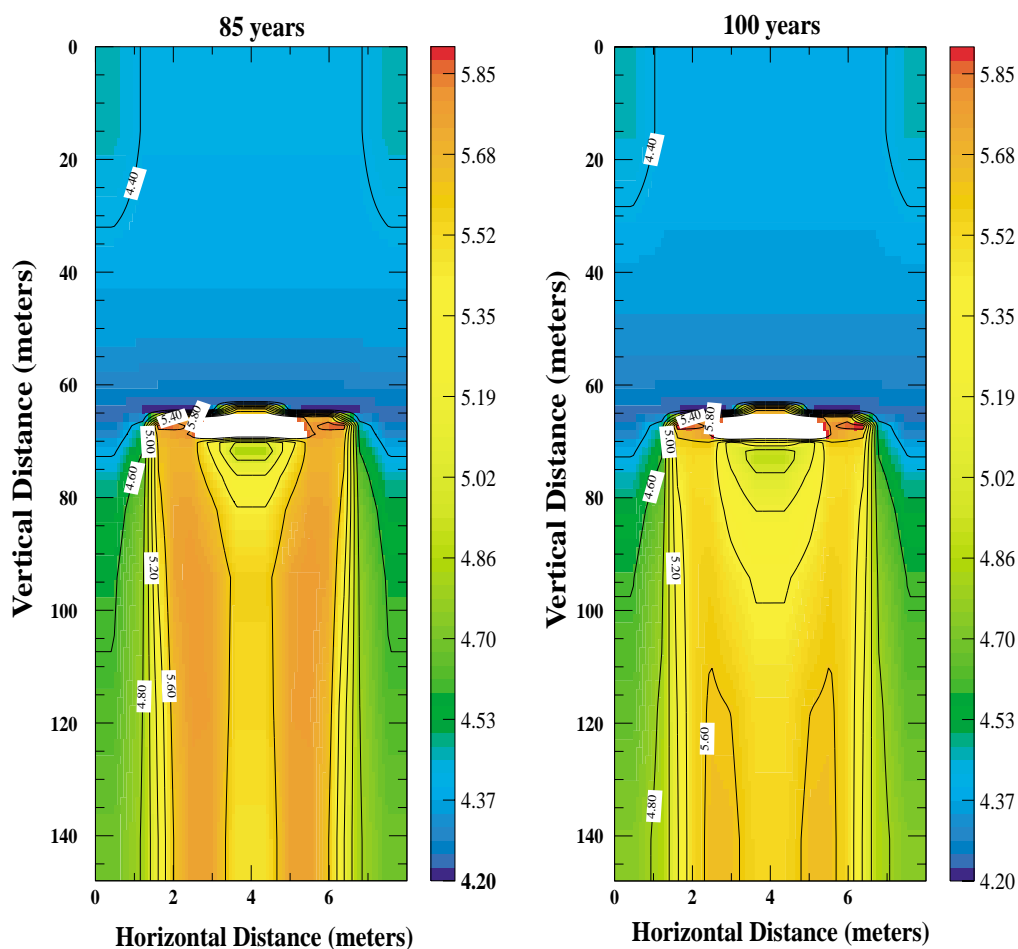


Figure 20. Cross section through a waste emplacement tunnel showing the concentration of bicarbonate in fracture water at 85 years and 100 years after repository. This and the following cross section are from the same location as that shown in Figure 19. The color bar scale is the same for both times and is the negative log of the concentration, in units of molality. See Figure 19 for further description of the geometry.

These results demonstrate that developing and operating a successful monitoring program for a high level nuclear waste repository must have knowledge of the temporal and spatial

progression of physical and chemical changes in order to successfully conduct useful measurements. This knowledge must include details of what chemical species are measurable and how they would change. These simulations show that some easily measured variables (e.g., dissolved calcium) would provide less useful indications of progressive change than certain other variables (e.g., HCO_3^- , CO_2 and SO_4^{2-}) that may be more difficult to measure, but accurate measurement of which would provide more robust information.

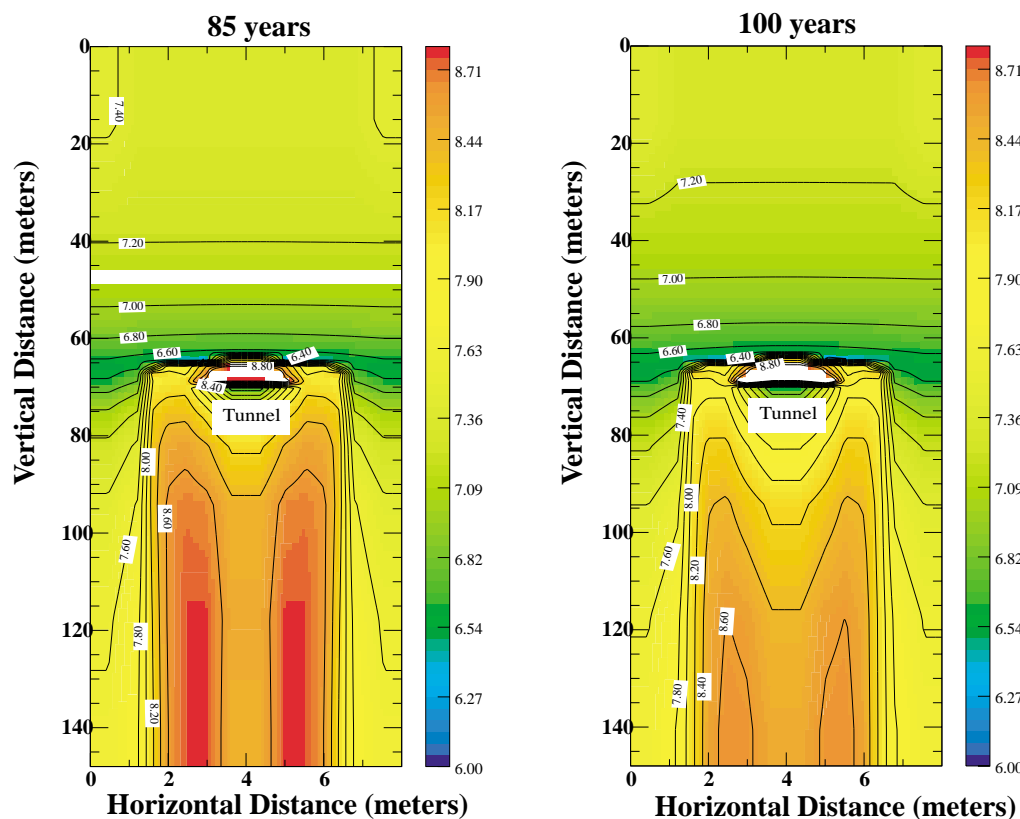


Figure 21. Cross section through a waste emplacement tunnel showing the CO_2 gas pressure in fractures at 85 years and 100 years after repository. The color bar scale is the same for both times and is the negative log of the pressure, in units of pascals. See Figure 19 for further description of the geometry.

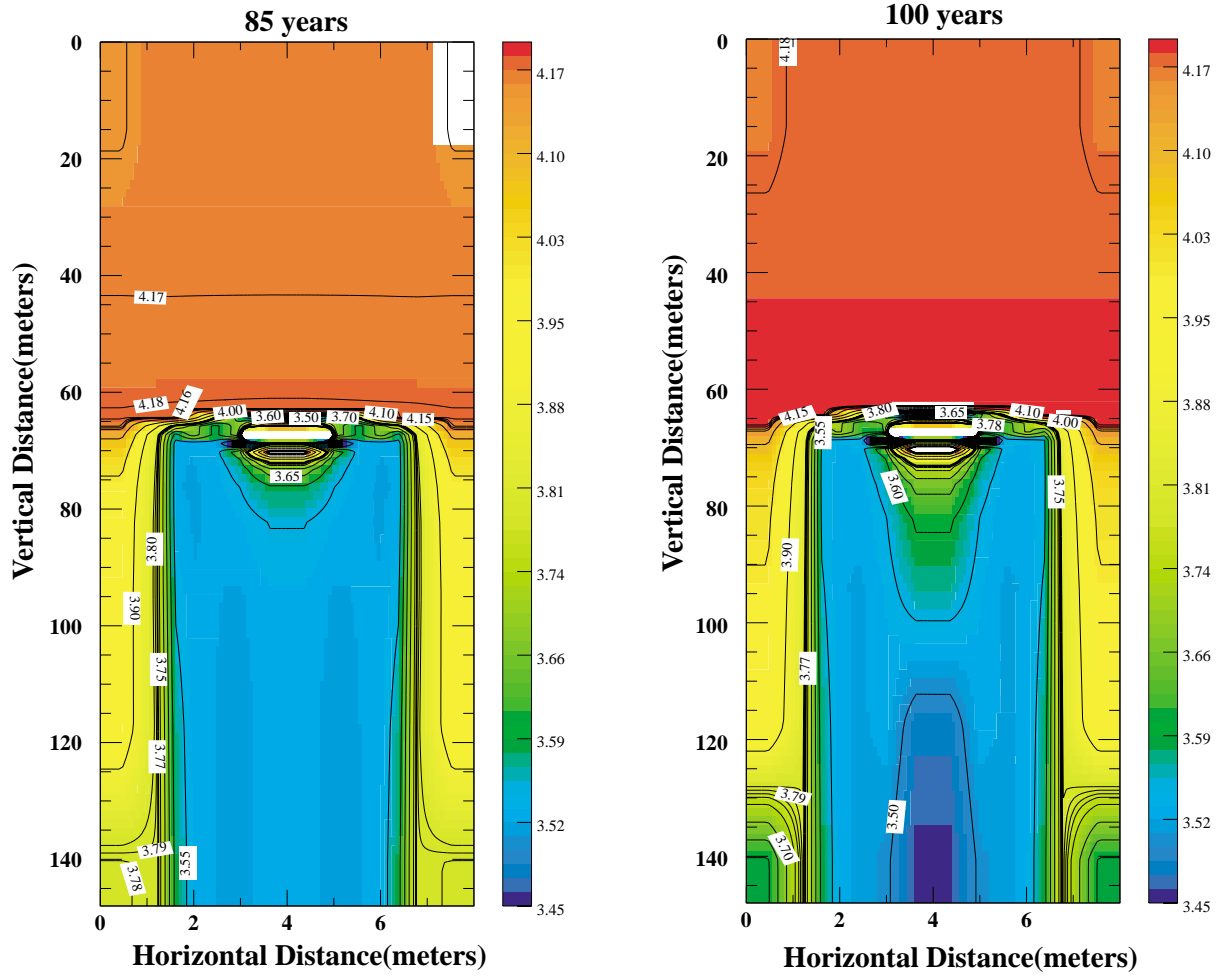


Figure 22. Cross section through a waste emplacement tunnel showing the concentration of sulfate in fracture water at 85 years and 100 years after repository. This cross section represents conditions 65 meters along the x-axis of Figure 17. The color bar scale is the same for both times and is the negative log of the concentration, in units of molality. See Figure 18 for further description of the geometry.

Other Applications

NUFT-C has been applied to several other studies concerning fluid movement and chemical processes within the Earth's crust (e.g., subsurface carbon sequestration and other nuclear waste disposal programs). There exists, in addition to these applications, a broad spectrum of possible applications of this code, but space limitations prevent detailed discussions of them. However, one additional application, significant for fossil fuel and geothermal energy production, is particularly relevant and worth mentioning.

We have conducted simulations in which we have modeled the thermal and geochemical evolution of a deep sedimentary basin. We selected this geological system because it has counterparts in both the oil and gas energy industry, as well as in low temperature geothermal systems. The basin we considered was seven kilometers deep and 12.5 kilometers on a side, and was assumed to be bounded by impermeable fault gouge. The basin was filled with a coarse, dirty sandstone, with low permeability shale layers alternating with coarse sand within 1 kilometer of the surface. The simulation was carried out to establish the type of circulation pattern that would evolve under conditions of a low thermal input that was localized within a 1 sq. km. area near the center bottom of the basin. The heat source was slightly offset from the center line of the basin, in order to consider the effects of asymmetry. The purpose of these simulations was also to determine the magnitude of change of porosity evolution, and the nature and magnitude of mineralogical changes with time.

For the conditions in this system, a complex flow regime developed, which is best visualized by considering temperature variability. Within the deeper levels of the basin there developed a double convection cell, below the less permeable shale layers, while a multitude of small convection cells developed in the rock units above the deepest shale layer (Figure 23). These contrasting flow patterns reflect the different relative values of the physical properties that control convective flow, in this case the relative permeabilities, the thermal properties of the rock, and the properties of the convecting fluid.

Mineralogical change was dominated by dissolution, resulting in a net increase in porosity throughout the basin, despite precipitation of numerous secondary phases. The greatest porosity change was in the region immediately above the heat source, where porosity increased by 7%, even with precipitation of numerous secondary minerals. In this simulation, the effects of porosity change on fluid flow were minimal.

The distribution pattern of secondary minerals generally follows that expected for this low temperature mineral suite. However, of particular interest is the extent to which fluid composition influences the occurrence of various mineral species. Consider, for example, the contrast between the distribution patterns for the two zeolites Ca-rich mordenite ($\text{Ca}_{0.5}\text{AlSi}_5\text{O}_{12} \cdot 4\text{H}_2\text{O}$) and natrolite ($\text{Na}_2\text{Al}_2\text{Si}_3\text{O}_{10} \cdot 2\text{H}_2\text{O}$). The former exactly mimics the temperature isotherms, consistently appearing at temperatures in excess of ca. 100°C, and increasing in abundance as temperature increases (Figure 24). Natrolite (Figure 25) although

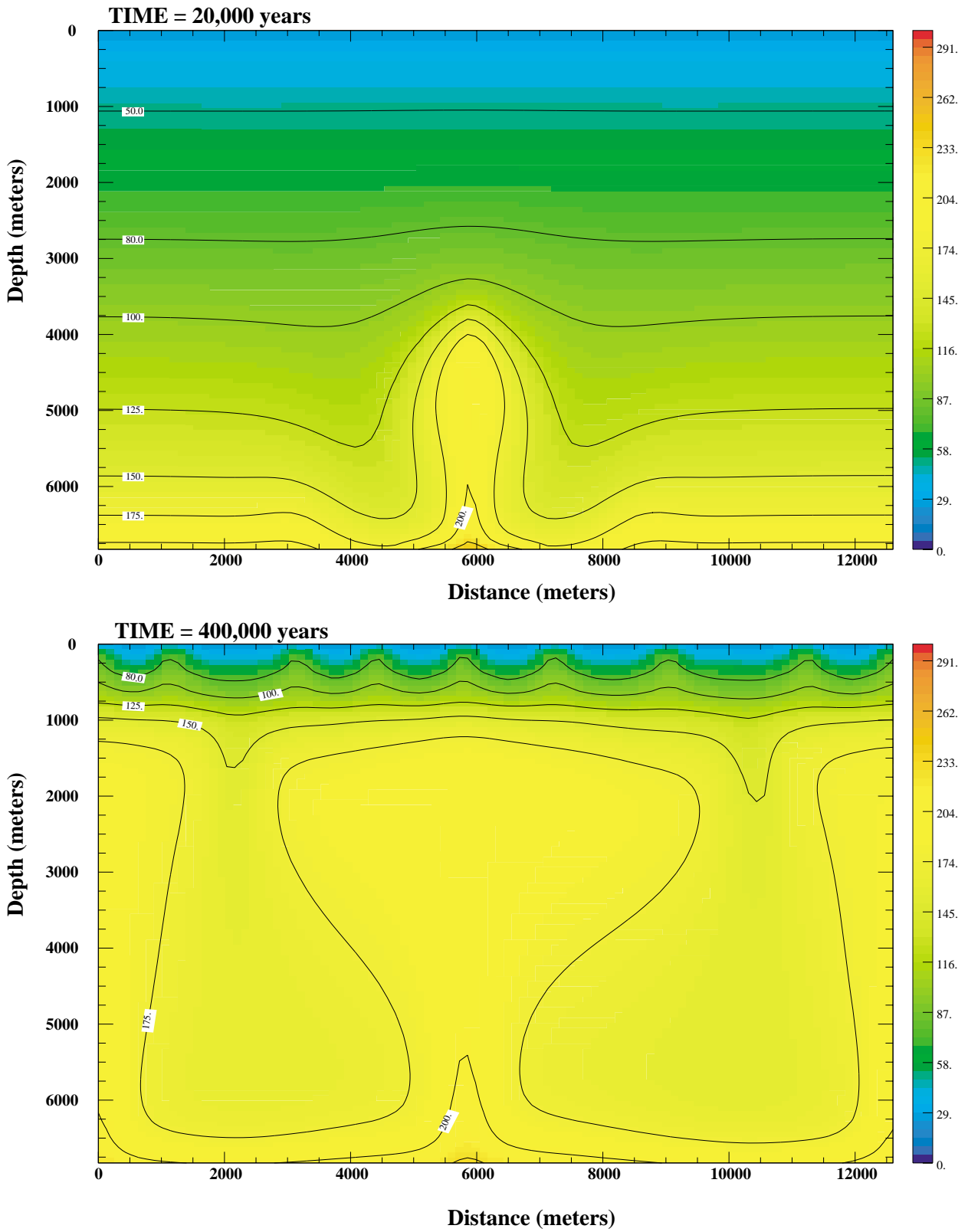


Figure 23: Temperature distribution at 20,000 and 400,000 years. Color scales are the same for both time periods

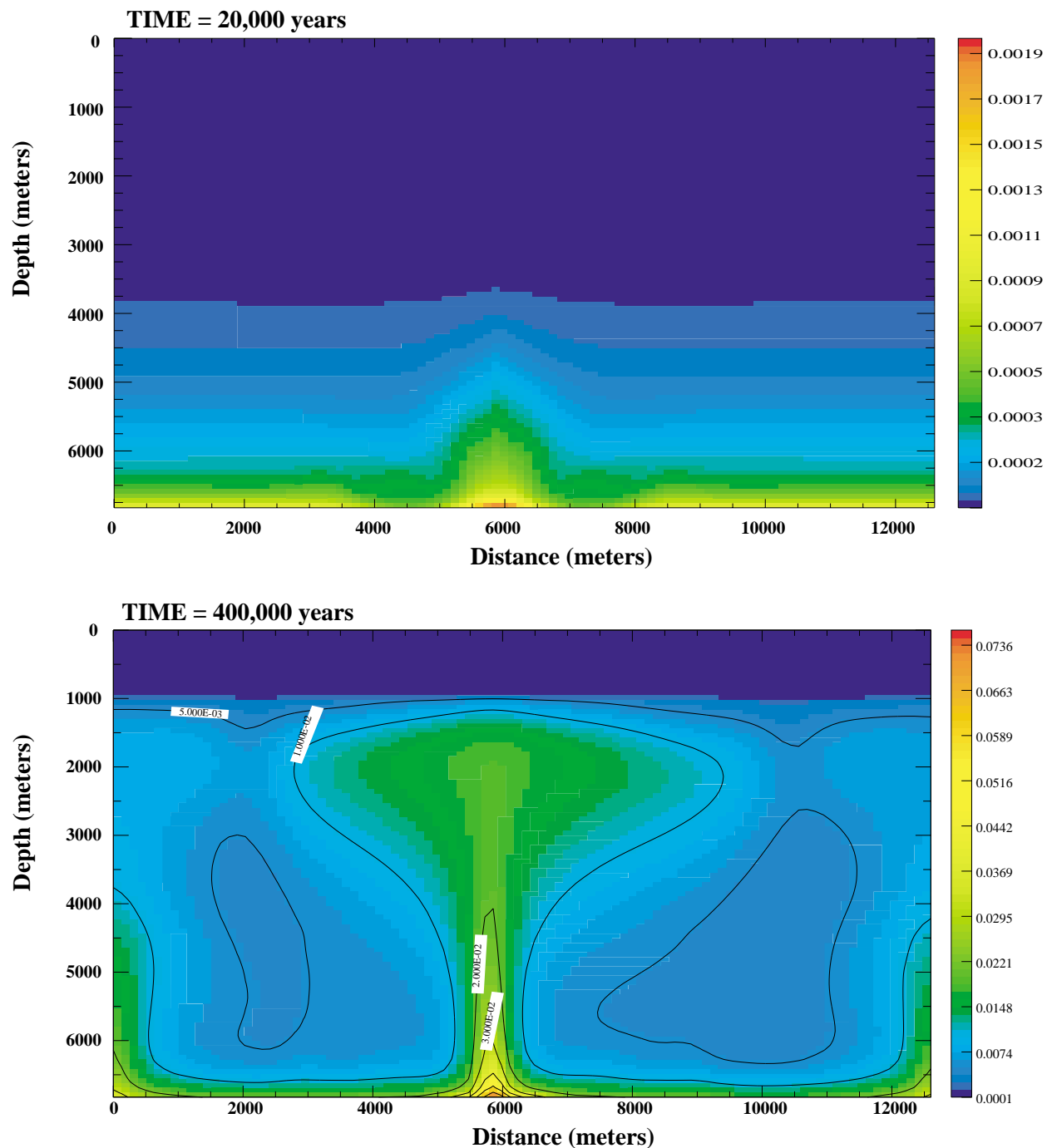


Figure 24. Mordenite distribution at 20,000 and 400,000 years. Color values represent volume fraction of mordenite. Note the difference in color scale values for the two time periods.

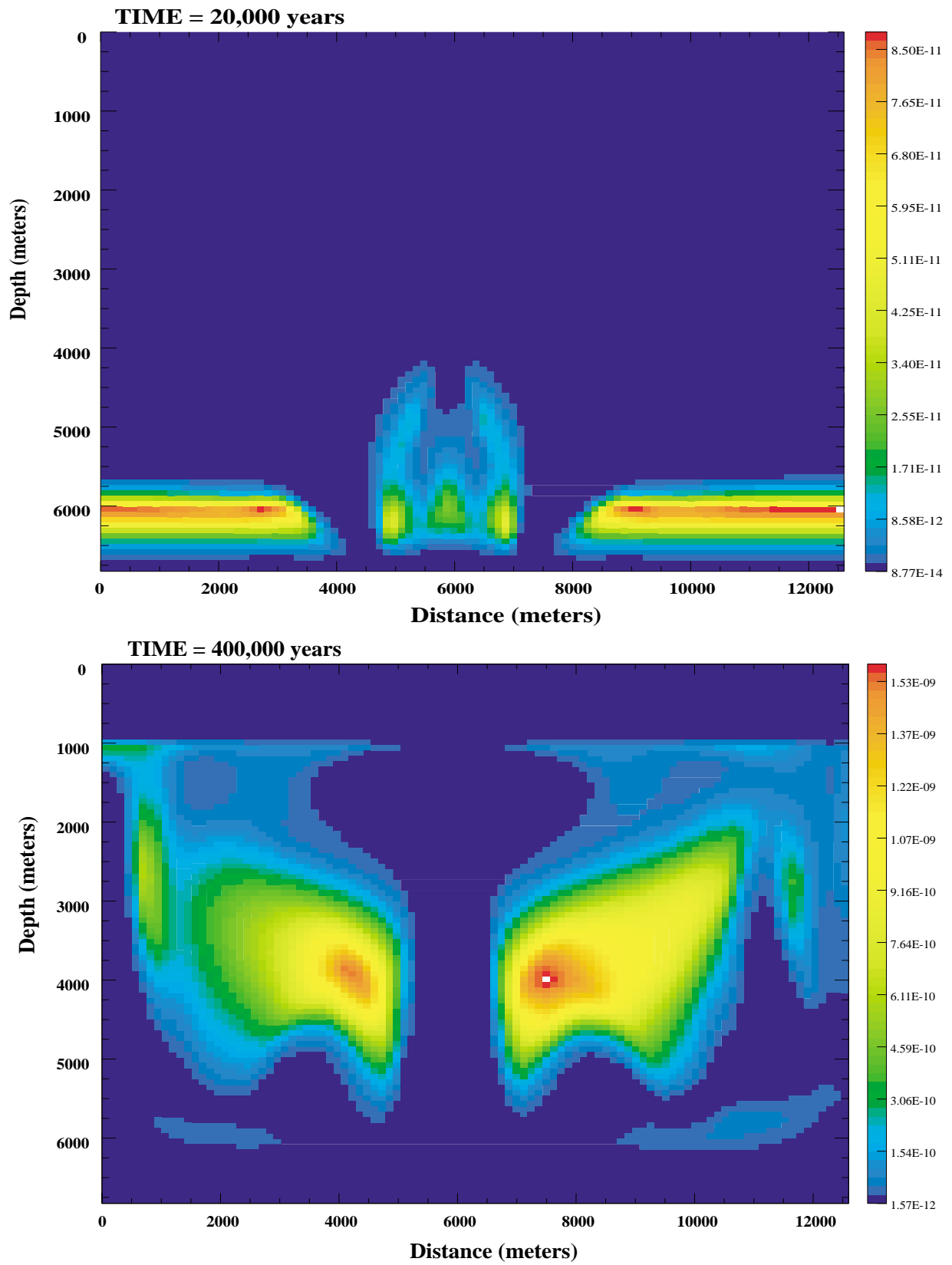


Figure 25. Natrolite distribution at 20,000 and 400,000 years. Color scale represents the volume fraction of natrolite. Color scale values for the two time periods are different.

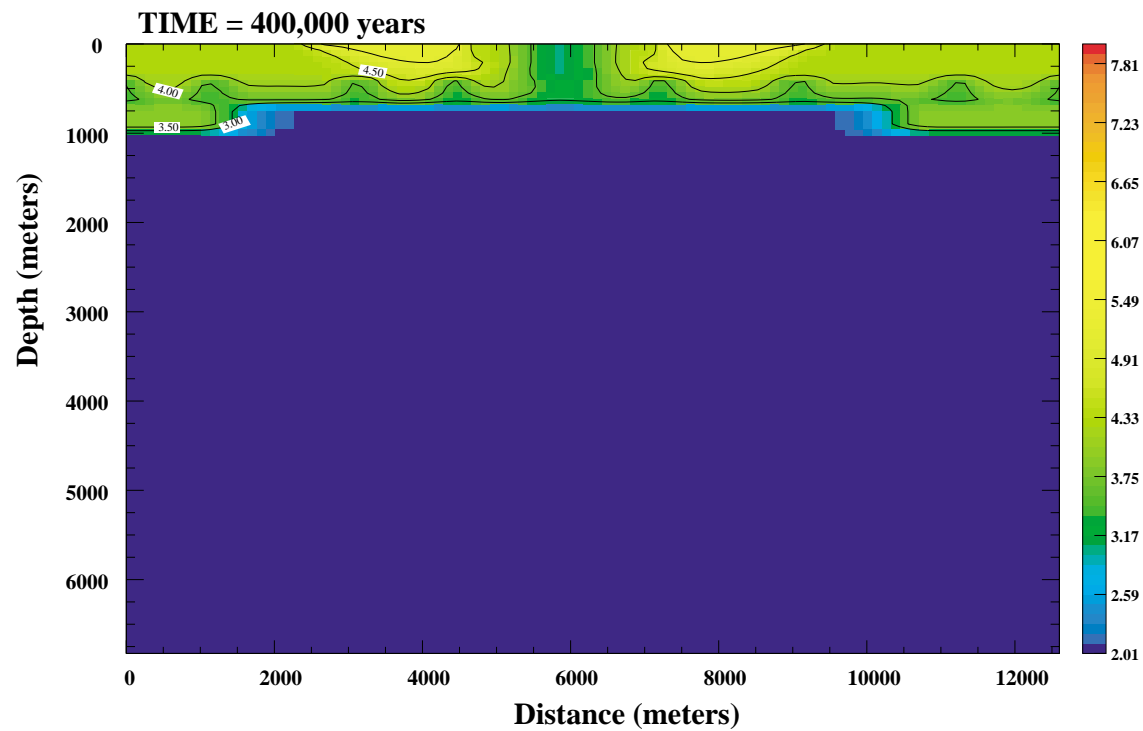
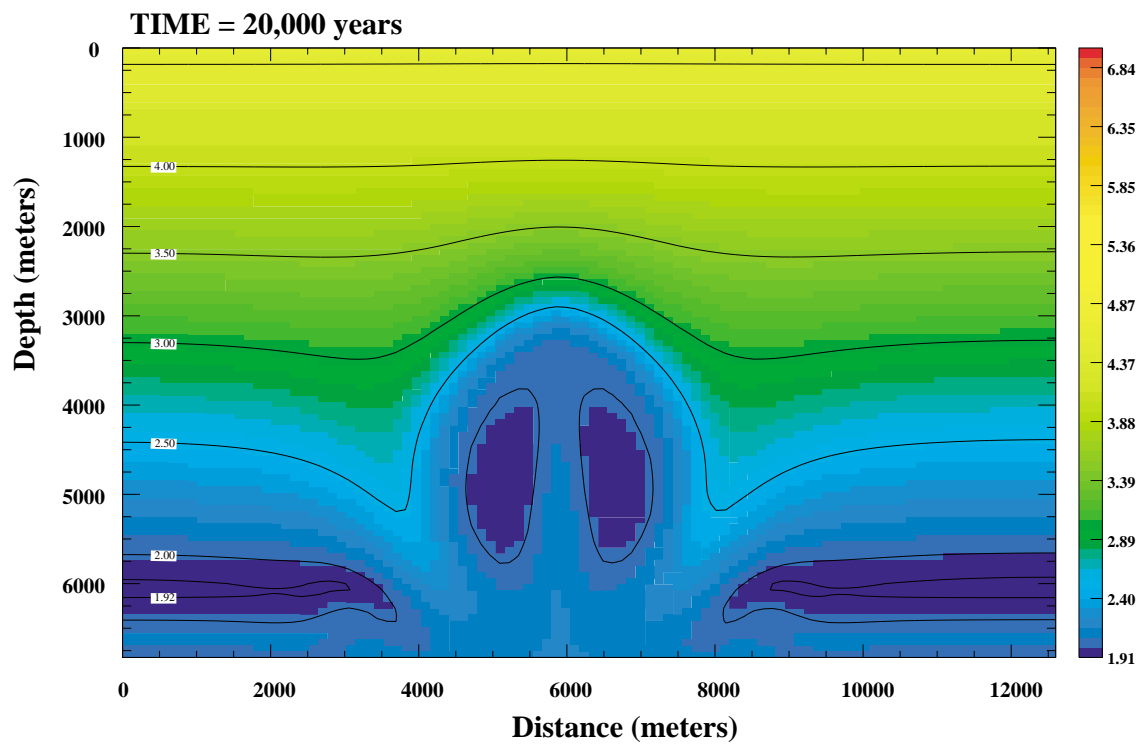


Figure 26. Dissolved Na^+ concentrations at 20,000 and 400,000 years. Color scale represents the negative log of the Na^+ molality. Note the difference in the color scale values for the two time periods.

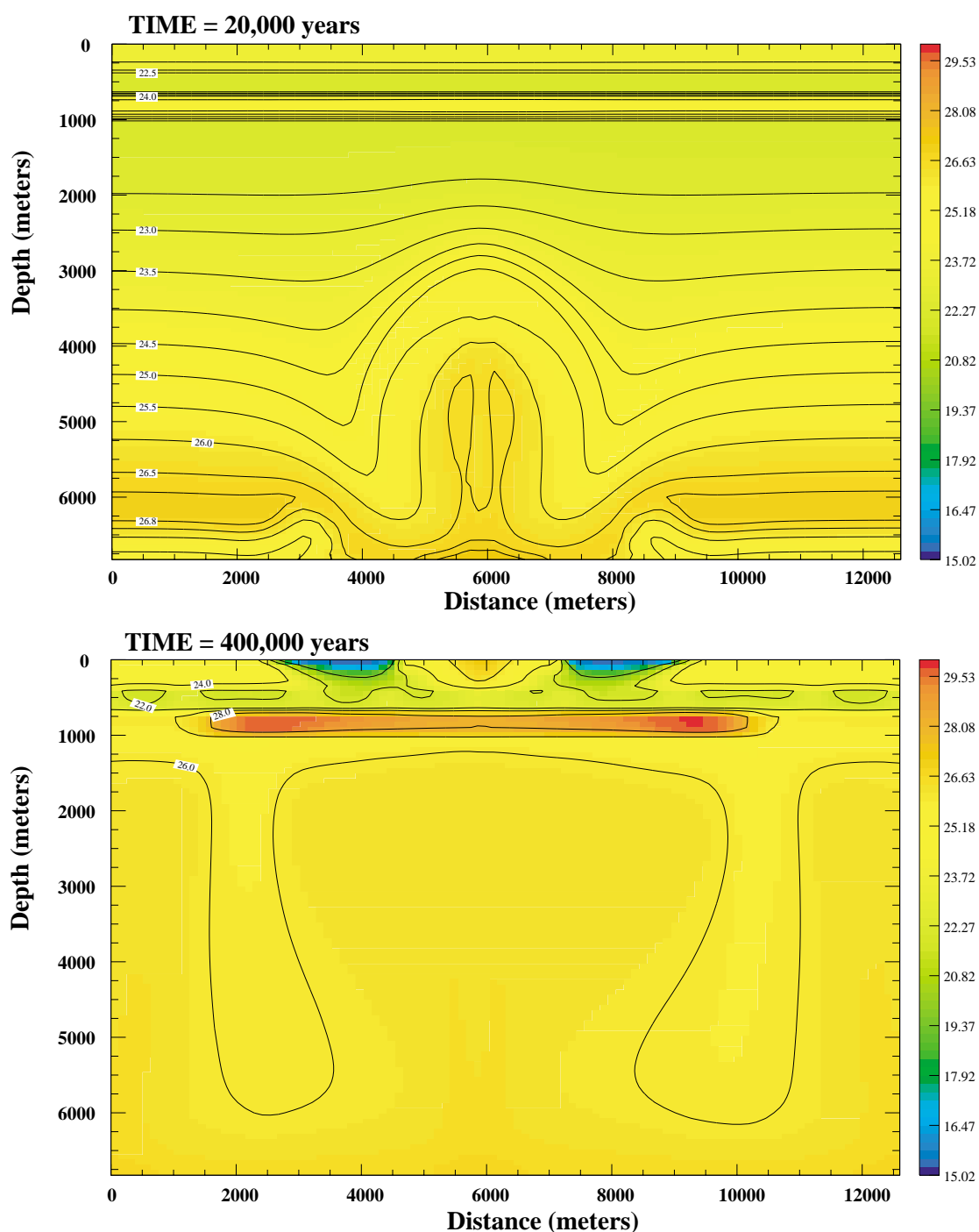


Figure 27. Dissolved Al^{+++} concentrations at 20,000 and 400,000 years. Color scale represents the negative log of the Al^{+++} molality. Note that the color scales are the same for the two time periods.

constrained to fall within the temperature interval 150°C to 170°C , is also strongly correlated with those regions in which Na^{+} (Figure 26) and Al^{+++} (Figure 27) are most concentrated. Note, also, that natrolite abundances are so low as not to be detectable were this a natural system. Nevertheless, the distribution of this mineral demonstrates an important principle regarding the relationship between mineral occurrences and fluid composition.

Also evident in these simulations is how quickly mineral distribution patterns can change with time, reflecting the dynamic character of the flow fields as heat is added to the system. This demonstration of fluid-rock interaction in this setting provides important insight into the complex interactions that control the evolution of secondary mineral and porosity development. Depending upon the need at hand, this simulation capability can be used to interpret the evolutionary history of a basin, as a means for guiding further exploration, or as a predictive tool, to understand how the system may respond if it is perturbed by natural (e.g., faulting or changes in surface recharge), or human (e.g., deep well injection of wastes or extraction of natural resources) events.

VI. SUMMARY

Successful completion of this Strategic Initiative has resulted in the development of a unique simulation capability, NUFT-C, for Lawrence Livermore National Laboratory. This capability allows high resolution modeling of complex coupled thermal-hydrological-geochemical processes in the saturated and unsaturated zones of the Earth's crust. The code allows consideration of virtually an unlimited number of chemical species and minerals in a multi-phase, non-isothermal environment. Because the code is constructed to utilize the computational power of the tera-scale IBM ASCI computers, simulations that encompass complex chemical system and large rock volumes can now be done quickly, and not sacrifice spatial or temporal resolution.

The code has been validated by comparing results of simulations to laboratory-scale experiments, other benchmark codes, field scale experiments, and observations in natural systems. The results of these exercises demonstrate that the physics and chemistry embodied in the code accurately represents the state-of-the-art in representing these processes, and that the conceptualization of the models used in the simulations honors the primary processes that are controlling these systems.

Application of the code to a wide range of important and strategic problems has been undertaken. Particularly significant are results obtained concerning the evolution of a potential high level nuclear waste repository at Yucca Mountain, Nevada. In these simulations, the results suggest that fluid movement and chemical changes will tend to be of greatest extent around the sides of the waste emplacement tunnels, thus minimizing the potential for seepage of water and dissolved salts into the tunnels from the tunnel crown. The results also indicate that the short term response of the geological system to waste emplacement will be complex and rapid, and will be most readily detected and monitored in regions immediately below waste emplacement tunnels. However, not all chemical species respond similarly, with some readily and commonly measured aqueous species changing insignificantly during a typical monitoring period. It is thus evident that a successful monitoring program of repository performance during the early stages of the operational period would greatly benefit by coordinating design and execution of sampling strategies with a simulation tool such as the one developed here. Such an approach would allow efficient and cost-effective sampling strategies, and would ease interpretation of what will surely be complex and massive data sets.

VII. ACKNOWLEDGEMENTS

Throughout the execution of this effort, discussions with numerous people aided effective development of this capability. Particularly significant were discussions with Drs. Dennis Bird and Phil Neuhoff at Stanford University, and Dr. George Barr at Sandia National Laboratory in Albuquerque. Consistent encouragement and guidance from Dr. Leland Younker is gratefully acknowledged. This effort would not have succeeded without the unfailing support of Dr. William Lokke, whose comments and thought-provoking criticism helped us overcome major hurdles. Comments and reviews from the external reviewers, Drs. Dennis Bird, Kenneth Eggert and Antonio Lasaga are gratefully acknowledged. We would also like to express our thanks to the various members of the LDRD review panels whose critical oversight contributed to the success of this project.

VIII. REFERENCES

- Balay, S., Gropp, W., McInnes, L.C., Smith, B., 1997, "PETSc 2.0 Users Manual", *Argonne National Laboratory, Argonne, IL*, ANL-95/11-Revision 2.0.21.
- Browning, L., Murphy, W.M., Leslie, B.W., Dam, W.L., 2000, Thermodynamic interpretation of chemical analyses of unsaturated zone water from Yucca Mountain, Nevada, in, *Scientific Basis for Nuclear Waste Management XXIII*, edited by R. W. Smith and D.W. Shoesmith (Mater. Res. Soc. Proc. 506, Warrendale, PA), pp.237-242.
- Johnson, J.W., and Lundeen, S.R., 1994a, Jewel: A graphical-user interface for generating custom GEMBOCHS thermodynamic datafiles for use with geochemical modeling software: LLNL-YMP Milestone report MOL63, 23 p.
- Johnson, J.W., and Lundeen, S.R., 1994b, GEMBOCHS thermodynamic datafiles for use with the EQ3/6 software package: LLNL-YMP Milestone report MOL72, 99 p.
- Johnson, J.W., and Lundeen, S.R., 1995, Facet: A graphical-user interface for viewing and updating the GEMBOCHS thermodynamic database: LLNL-YMP Milestone report MOL208, 28 p.
- MPI, 1995. MPI: A Message-Passing Interface Standard. Message Passing Interface Forum, June 12, 1995.
- MPI-2, 1997. Extensions to the Message-Passing Interface. Message Passing Interface Forum, July 18, 1997.
- Nitao, J. J., 1998, "Reference Manual for the NUFT Flow and Transport Code, Version 2.0," *Lawrence Livermore National Laboratory, Livermore, CA*, UCRL-MA-130651.
- Steeffel, C.I., 2000, New directions in hydrogeochemical transport modeling: Incorporating multiple kinetic and equilibrium reaction pathways. *Computational methods in Water resources XIII*, Bentley, et al., eds. Calgary, Canada. 25-29 June, 2000. A.A. Balkema Publishing, Rotterdam. Pp. 331-338.
- Steeffel, C.I. and Yabusaki, S.B., 1996, OS3D/GIMRT, Software for modeling multi-component multidimensional reactive transport. User's Manual.
- Yang, I.C., Rattray, G.W., and Yu, P., 1996, United States Geological Survey WRIR 96-4058.
- Yang, I.C., Yu, P., Rattray, G.W., Ferarese, J.S. and Ryan, R.N., 1998, United States Geological Survey WRIR 98-4138.
- YM Document MDL-NBS-HS-000001, 2000, Drift-Scale Coupled Processes (Drift-Scale Tset and THC Seepage) Models. Yucca Mountain Project.

IX. PUBLICATIONS

Bildstein, O. and Steefel, C.I., 2001, The role of pore pressure solution in fracture healing: A multi-scale reaction-flow modeling approach. *Geofluids*, to be submitted.

Glassley, W. E., Simmons, A. M. and Kercher, J. R., 2001, Mineralogical heterogeneity in fractured, porous media and its representation in reactive transport models . *Applied Geochemistry*, in press.

Glassley, W. E., Nitao, J.J., Grant, C.W., and Boulos, T.N., 2000, Modeling thermal-hydrological-chemical coupled processes in the vadose zone using massively parallel, high performance computers. Abs., Geological Society of America Annual Meeting, Reno, Nevada.

Glassley, W. E., Nitao, J.J., Grant, C.W., Boulos, T.N., Gokoffski, M. O., Johnson, J. W., Kercher, J. R., Levatin, Jo Anne and Steefel, C. I., 2000, High Resolution, 3-Dimensional Coupled Thermal-Hydrological And Geochemical Simulations For Repository Performance Assessment And Post-Closure Monitoring. Materials Research Society Annual Meeting 2000, Sydney, Australia.

Nitao, J. J., and Glassley, W. E., 1998, "Modeled porosity modification in the near-field environment due to coupled thermal-hydrological and geochemical processes," *Scientific Basis for Nuclear Waste Management XX*, UCRL-JC-131163, 98-SI-004.